ESRF
NEWSLETTER

JULY 1996 EUROPEAN SYNCHROTRON RADIATION FACILITY N° 26

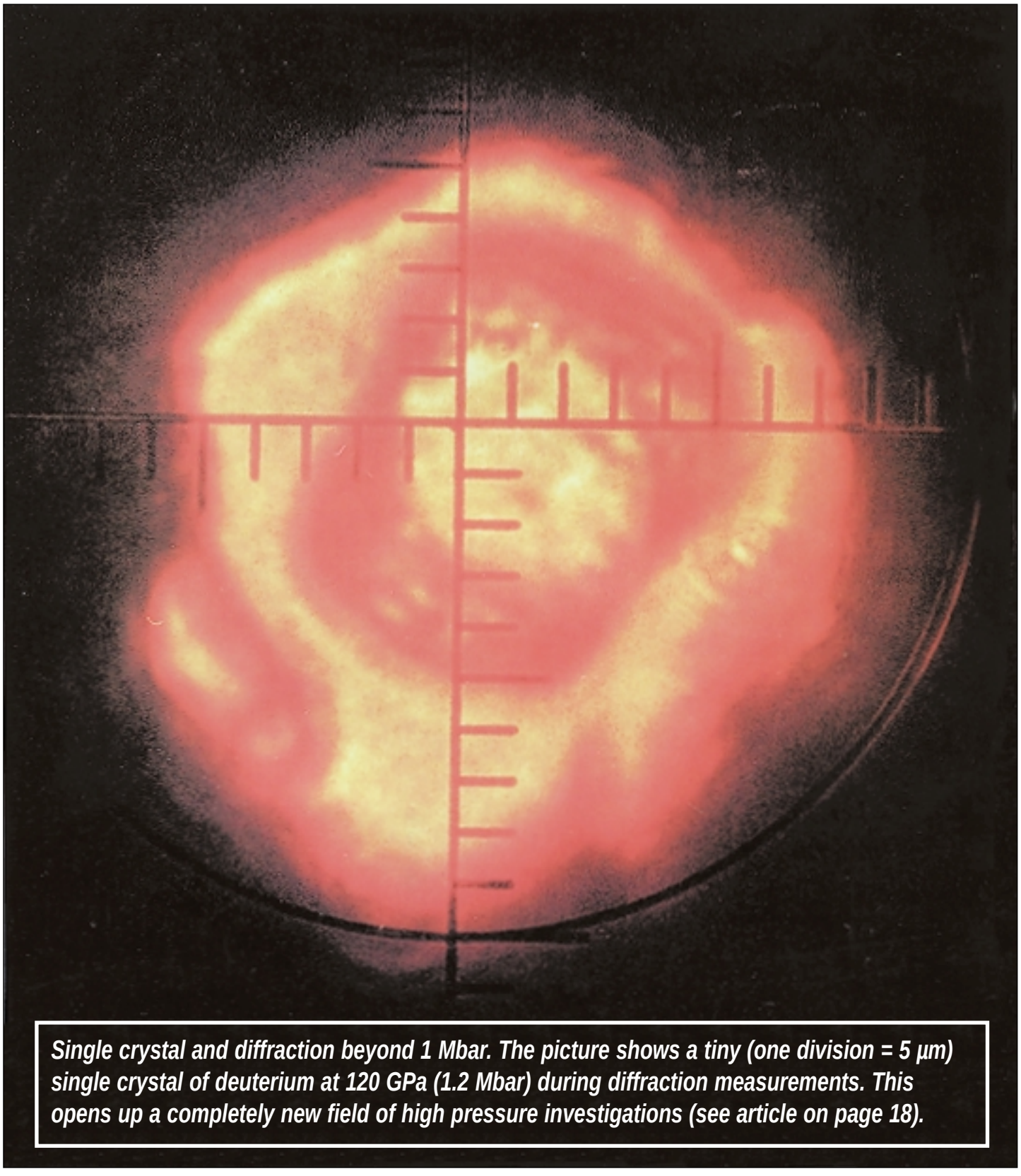

Single crystal and diffraction beyond 1 Mbar. The picture shows a tiny (one division = 5 µm) single crystal of deuterium at 120 GPa (1.2 Mbar) during diffraction measurements. This opens up a completely new field of high pressure investigations (see article on page 18).

ISSN 1011-9310

CONTENTS

EDITORIAL
About the Newsletter…, PAGE 2.

NEWSLETTER IN BRIEF
Highlights from the 24th meeting of the ESRF Council, PAGE 3.
New brilliance delivered to users!, PAGE 3.
Goodbye to… Jean-Louis Laclare, PAGE 3.
News for users, PAGE 4, R. Mason.
Visit of the Italian Minister of Research, PAGE 5.
HERCULES, PAGE 6.
CERN school on synchrotron radiation and free electron lasers, PAGE 8.
APS/Spring-8/ESRF collaboration, PAGE 8.

EXPERIMENTS REPORTS
Low-frequency dynamics probed with coherent X-rays, PAGE 10, G. Grübel, D. Abernathy, T. Thurn-Albrecht, W. Steffen, A. Patkowski, G. Meier and E.W. Fischer
Resonant inelastic scattering using circularly polarised soft X-rays, PAGE 12, L. Braicovich, N. B. Brookes, C. Dallera, G. Ghiringhelli and J. B. Goedkoop.
Ultra small-angle X-ray scattering, PAGE 15, O. Diat, P. Bösecke, O. Dhez, J. Gorini and J. Lambard.
Single crystals above one megabar: progress report, PAGE 18, P. Loubeyre, R. LeToullec, D. Häusermann and M. Hanfland.
X-ray inelastic scattering with nuclear resonance techniques, PAGE 20, A. I. Chumakov, A. Q. R. Baron, R. Rüffer, H. Grünsteudel and H. F. Grünsteudel.
Phase equilibria of charged lamellar phases, PAGE 22, F. Ricoul, M. Dubois, A. Vandais, J-P. Noel, T. Zemb, M. Lefevre, D. Plusquellec and O. Diat.
Mosaic spread measurements of space-grown and of earth-grown protein crystals, PAGE 27, J.-L. Ferrer, J. Hirschler, M. Roth and J. C. Fontecilla-Camps.

INSTRUMENTATION REPORTS
Capillary optics, PAGE 30, P. Engström, A. Rindby and L. Vincze.
Jitter-free accumulating streak camera with 100 femto-second time resolution, PAGE 32, G. Mourou, G. Naylor, K. Scheidt and M. Wulff.

EVENTS
Atomiades (Feb. '96), PAGE 36.
Visit of the Italian Minister of Research (May '96), PAGE 36.
ESRF users meeting: «Science at the ESRF» (Nov. '96), PAGE 36.

Photography by:
C. Argoud, C. Jarnias, Studio de la Revirée, S. Turner.

ABOUT THE NEWSLETTER...

The ESRF Newsletter is published three times per year and is distributed free of charge.
If you wish to receive it regularly, please fill out the form below and mail it or fax it to the following address:

ESRF • Information Office
BP 220 • F-38043 Grenoble Cedex 9 • FRANCE
Fax: +33 76 88 24 18

Name: .....

Company name: .....

Address: .....

PO box: .....

Country: .....

Highlights from the 24th meeting of the ESRF Council

The 24th meeting of the ESRF Council was held in Grenoble on 17 June 1996.

Long-term Planning

The Council welcomed the document submitted as extremely helpful in the development of a long-term strategy for the ESRF. The Council agreed to give priority to the enhancement of the source and the beamlines by refurbishment and technical developments rather than to an extension of capacity by the addition of more beamlines. However, most delegations expressed reservations about any increase in the amount of annual contributions beyond the present level.

Management will prepare a revised version of the strategy paper together with a more detailed five year programme and multi-annual financial estimates, taking into account the comments made, to be submitted to the Science Advisory Committee, the Administrative and Finance Committee and again to the Council at its meeting in November 1996.

Joint Structural Biology Group (JSBG)

The Council approved the establishment of an ESRF-EMBL joint structural biology group. A draft agreement between ESRF and EMBL will now be finalised and submitted for approval.

Budget for 1997

The Council, taking into account the difficult budgetary situation anticipated in some Contracting Party Countries, adopted 400 MFF as the planned level of new contributions from members to the 1997 budget. The Council expected this budget to include the necessary provisions for completing the last beamlines of the set of thirty envisaged in the ESRF Convention by the end of 1998. Some delegations indicated that this level of contributions was subject to the availability of funds in their national budgets.

In view of the prevailing uncertainty of the resources which will actually be available and the prospects of additional income, the Council asked the Management to also prepare an optional budget for 1997 based on the previous planning figure of 408,5 MFF on new contributions from Members.

Appointments from Non-contracting Party Countries

The Council adopted as a guideline that

- the overall proportion of staff who are not a national of one of the contracting-party countries, should not exceed about 5 % and
- the corresponding proportion of staff scientists working on the beamlines (including post-doctoral fellows and thesis students) should not exceed about 10 %.

Changes in the Directorate

The Council decided that the posts of the Machine Director and the Research Director (succession of C.I. Brändén) be advertised with deadline 15 September 1996.

New brilliance Delivered to Users!

As from May 1996, the horizontal and vertical emittances offered during users' shifts are $3.7\ 10^{-9}$ mrad and $1.5\ 10^{-11}$ (0.4 % coupling). This has allowed us to reach a brilliance of $1.5\ 10^{20}$ ph/s/mm^2/mrad^2/0.1%BW with an undulator of 3.2 m and a gap of 16 mm. The next goal is to obtain 6.10^{20} ph/s/mm^2/mrad^2/0.1%BW with a 5 m undulator and a gap of 10 mm.

The decrease of the vertical emittance has already shown dramatic effects on phase contrast imaging.

Y. Petroff

Goodbye to... Jean-Louis Laclare

J.-L. Laclare, the most senior member of the ESRF's Directorate (having started on 1 April 1986 as Project Director and continued since 1 September 1995 as Machine Director) has decided to leave the ESRF in August in order to meet a new challenge: the construction of the French synchrotron radiation source SOLEIL.

Although the construction and further development of the ESRF Machine is the result of the teamwork of staff from several Divisions, the driving force personified by J.-L. Laclare was the decisive factor to push the performance of the source by orders of magnitude beyond initial specification and to reach the presently outstanding reliability in operation.

For his new task we wish J.-L. Laclare the same success he had at the ESRF.

News for Users

New Beamlines open for Users

In May 1996, three new beamlines successfully carried out their first series of user experiments. They are BM16 for powder diffraction, ID19 for topography and high-resolution diffraction, and ID20 for magnetic scattering. This brings the number of beamlines now regularly scheduling experiments to 20 ESRF public beamlines and 4 Collaborating Research Group (CRG) beamlines. During late summer 1996, two more beamlines, ID30 for high pressure, and ID1 for anomalous scattering experiments, are expected to begin user operation.

Beamline Numbering

Members of ESRF committees and users will have noticed that the beamline numbers were modified recently (see *Newsletter* No. 25, p.43). This change was made to simplify the numbering of beamlines, which are now named either IDxx if the source is an insertion device, or BMxx if the source is a bending magnet. The numbers follow consecutively around the ring, and thus indicate the location of the beamline. The letters A or B attached to the ID number, used for ID12A and ID12B, for example, indicate the experimental station, and in this particular case replace the former BL6 and BL26. More exotic names remain, however, and you will come across users referring to TROIKA and GILDA, for example.

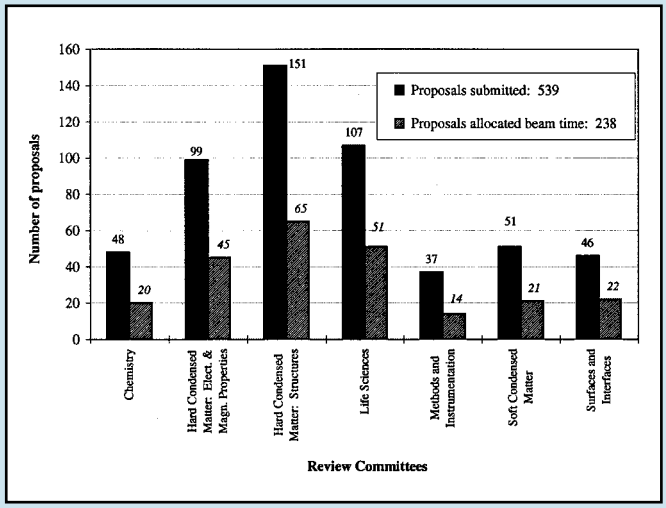

Fig. 1 Proposals submitted and allocated beam time, per Review Committee.

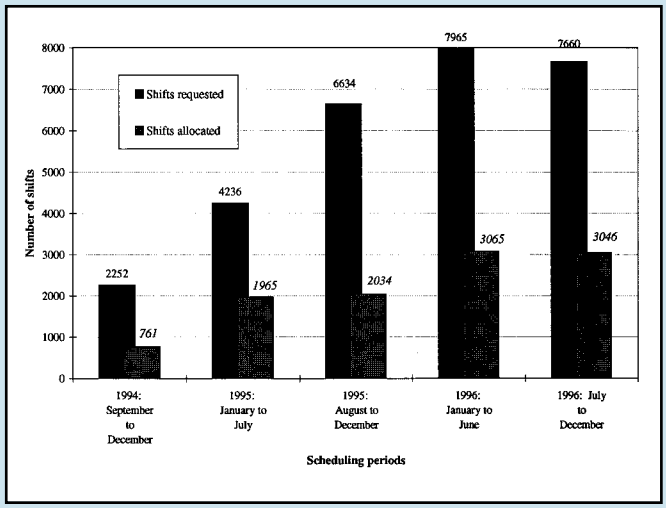

Fig. 2: Total number of shifts of beam time requested and allocated, per scheduling period.

Results of the Proposal Review March - April 1996

The Review Committees, whose members are appointed for two years with the possibility of an extension of one year, were recently restructured, and new members appointed. Furthermore, in view of the large number of proposals arriving in the area of hard condensed matter, this committee was split in two, to review applications relating to structures on the one hand, and electronic and magnetic properties on the other.

The new Review Committees met at ESRF on 29 and 30 April 1996 to assess the 539 proposals submitted for beam time between August and December 1996. The Committees graded the proposals on the basis of their scientific merit, and recommended the number of shifts to be allocated to each experiment. Following a final feasibility check, and review by management, 238 proposals totalling 3046 shifts were allocated beam time. Fig. 1 shows the results of these allocations per Review Committee, while Fig. 2 shows the number of shifts allocated compared with shifts requested, per scheduling period, since the beginning of user operation. It should be noted that the second scheduling period during each year is slightly shorter than the first, and this accounts for the lower number of shifts allocated and scheduled during the second half of the year. Considered overall therefore, 44% of proposals were successful this round, compared with an average of 45% over previous rounds.

Operating Schedule

The operating schedule and beam modes for the second half of 1996 are now set. There will be three runs of 6 to 7 weeks separated by two 10-day shutdowns. During each run period, one to two days per week are devoted to maintenance tasks and machine physics studies. Long shutdowns are planned in July, and from 18 December 1996 to 17 January 1997.

Beam will be delivered in an increasing number of exotic modes which, during the next six months, include single bunch, 16 bunch, 1/3 filling, and two types of "hybrid" mode. The hybrid modes combine 1/3 filling with one or two single bunches. User teams are therefore strongly encouraged to discuss the scheduling of their experiments with the beamline scientist at a very early stage, to ensure as far as possible that beam characteristics are optimal.

We remind readers that information including characteristics of the source and beamlines, details of operation periods and beam modes, together with application forms are available on the World Wide Web (WWW) at the ESRF address:

http://www.esrf.fr.

R. Mason

THE DEADLINE FOR PROPOSALS FOR BEAM TIME BETWEEN JANUARY AND JUNE 1997 IS 1 SEPTEMBER 1996

Visit of the Italian Minister of Research

On Friday 3 May 1996, Professor Salvini, Italian Minister of Research, visited the ESRF. He was welcomed by Professor Menzinger, Chairman of the ESRF Council, and Professor Petroff, Director General.

Professor Salvini met the Italian staff of the ESRF and inaugurated the two CRG beamlines GILDA and GRAAL.

GILDA is an Italian CRG beamline and GRAAL is a collaboration between Italian and French scientists.

Professor Salvini also met some Italian scientists in charge of ESRF beamlines.

HERCULES 1996

The sixth session of the HERCULES course (Higher European Research Course for Users of Large Experimental Systems) took place at the Maison des Magistères, CNRS Grenoble, from 26 February to 4 April 1996, with 64 participants from 17 countries (mostly European, but including participants from Indonesia, Ghana and Guatemala registered in European Universities):

• session A : 'Neutron and synchrotron radiation for physics and chemistry of condensed matter' with 44 full time participants and 4 part time participants

• session B: 'Neutron and synchrotron radiation for structural molecular biology' with 16 full time participants.

The course included lectures, practicals and tutorials as in previous years. In Grenoble most of the practicals were carried out on ESRF beamlines (including French and Italian CRG beamlines) and at the ILL. The collaboration of IBS, EMBL as well as CNRS and CEA-Grenoble was also greatly appreciated. Participants from session A carried out practicals at LURE (Orsay) and Laboratoire Léon Brillouin (Saclay).

The poster session at the Maison des Magistères (44 posters displayed) was one of the highlights of the course and allowed fruitful exchanges between participants and Grenoble scientists.

HERCULES 97 will follow next year with the same two parallel sessions from 17 February to 27 March. Session A will be more particularly centered on recent developments of neutron and X-ray spectroscopy.

Information and application forms will be available at the beginning of July.

HERCULES 1997

Higher **E**uropean **R**esearch **C**ourse for **U**sers of **L**arge **E**xperimental **S**ystems

Grenoble, 17 February - 27 March 1997

Session A:

«Neutron and synchrotron radiation for physics and chemistry of condensed matter»

Session B:

«Neutron and synchrotron radiation for structural molecular biology»

Information: Secrétariat HERCULES - M.-C. Simpson
CNRS - Maison des Magistères - 38042 Grenoble Cedex 9
Tel: 76 88 79 86 - Fax 76 88 79 81 - e-mail: simpson@mgstsrv.polycnrs-gre.fr

Deadline for application: 18 October 1996

The ESRF is seeking to recruit its

MACHINE DIRECTOR

THE FUNCTION :
The Machine Director is responsible for the operation and development of the three accelerators (comprising the light source) and for a series of insertion devices and beamline front-ends. He/she heads the Machine Division with responsibility for its annual budget (~60 MFF in 1996 excluding personnel costs) and staffing plans. He/she reports directly to the Director General of the Institute. There are about 70 staff members in the Division, but the Director can also call on the technical assistance of the Technical Services and Computing Services Divisions.

QUALIFICATIONS AND EXPERIENCE :
The successful candidate will have proven managerial skills including the handling of finance and personnel. With regards to the machine as such, the main goal of the Division is to maintain the excellent performance and availability levels attained in operation; this will be a priority for the new Director. In terms of absolute performance, the machine has greatly surpassed the original target specifications with a routinely served brilliance 100 times higher than expected. Such a machine should always be outstanding, and a series of upgrades are now being prepared for the medium term. The successful candidate will ideally have expertise in the field of operating a synchrotron light source, with experience at a third generation light source being highly appreciated.

The working language at the ESRF is English.
The initial contract will be for a five-year period.

If you are interested, please send your application by 15 September 1996 to the Chairman of the ESRF Council, B.P. 220, F-38043 Grenoble cedex 9, FRANCE

The ESRF is seeking to recruit a

RESEARCH DIRECTOR

THE FUNCTION:
Two Research Directors are in charge of the Experiments Division. This Division has the mission of designing, constructing and operating the beamlines. In addition to supporting the use of the beamlines by the scientific communities, it also executes programmes of scientific research and technical development using synchrotron radiation. The Research Director we are looking for will have a special responsibility for Life Sciences and Chemistry. He/she is expected to provide the scientific leadership of the Experiments Division in his/her area of responsibility. The Research Director will lead a synchrotron radiation related research programme of distinction, as well as advancing the state of the art in instrumentation and data acquisition. He/she will also be responsible for providing an efficient and up-to-date user service on the beamlines and maintaining a scientific review process for proposals and a fair allocation of beam time. The two Research Directors jointly have responsibility for the Experiments Division's annual budget (about 100 MFF in 1996 excluding personnel costs) and staffing plans. They report directly to the Director General of the Institute. There are currently about 200 staff members in the Division and the Directors can also call on the technical assistance of the Technical Services and Computing Services Divisions.

QUALIFICATIONS AND EXPERIENCE:
The selected candidate will be a leading scientist in the Life Sciences or Chemistry field although preference will be given to the former. He/she will have extensive experience of the application of synchrotron radiation in his/her chosen field proven by a substantial publication record. In addition, the Research Directors are required to have demonstrated leadership, management and administrative skills.

CERN School on Synchrotron Radiation and Free Electron Lasers - Grenoble, 22-27 April 1996

The ESRF was recently sponsor to a specialised CERN Accelerator School on Synchrotron Radiation and Free-Electron Lasers, held in Grenoble from 22 to 27 April 1996. The last school on this topic was held in Chester, UK, in 1989, and it was felt that the field had evolved so much since, in particular with the commissioning of third generation synchrotron light sources, that now was the right time for a new course.

Lectures were given on a wide range of subjects, including dynamics of electrons in rings, insertion devices, current limitations, lattices and emittances, lifetime, diagnostics and beam stability, linac and storage ring driver FELs, completed by seminars on such topics as scientific applications and industrial uses.

Out of the 60 students attending, about 40 came from various American, European and Japanese institutes, with the remainder being colleagues from the ESRF, eager to make good use of this opportunity of improving on their theoretical knowledge in accelerator physics.

One of the highlights of the week was undoubtedly the visit to the ESRF, where in addition to inspecting the tunnel and some of the beamlines, students were given the possibility of participating in tests on the machine.

APS / SPring-8 / ESRF Collaboration

The 3rd joint APS-ESRF-SPring-8 workshop to discuss and define collaboration projects took place at SPring-8 on April 15 and 16. A tour of the SPring-8 facilities left us impressed by the rapid progress that has been made in the construction of the machine.

During the workshop, the accelerators, insertion devices and beamlines of the three facilities were presented, followed by a discussion of technical development projects of common interest.

Projects of special interest for the beamlines were in the areas of optics, detectors, the use of robots in the experimental hutches, heat load problems as well as polishing of Be-windows and carbon filters. Among the concrete results achieved it can be mentioned that SPring-8 scientists will assist the ESRF to obtain diamond crystals and Si- ingots, which are in short supply world-wide, from Japanese companies. The ESRF will make beam time available and participate in SPring-8 tests of a new CCD-array detector and both the ESRF and SPring-8 will have the possibility to make in situ mirror tests at APS. It was also agreed that joint efforts should be made to define standard procedures to measure flux, brilliance and coherence and that the sharing of technical information between the three facilities should be improved.

The developments concerning the machine include RF BPMs (beam position monitors), XBPM, RF liners and the X-ray pinhole camera. Resonance, coupling and instabilities will also be subject of collaboration.

Prospective R&D in view of the 4th generation of light sources was discussed. It was agreed that it is essential that the three institutes remain in close contact and present a common view on the limits of synchrotron radiation sources. A panel of experts is being formed with this in mind.

There are topping-up tests scheduled at both APS and the ESRF and all three institutes are exchanging information as well as participating in the tests.

For all insertion device aspects, the ESRF has the leading role. The design, manufacture and optimisation techniques of standard insertion devices are now well understood and developed at all three institutes. One in-vacuum insertion device manufactured by SPring-8 is to be installed in one of the ESRF's straight sections in July '96 and conclusions of preliminary tests will be drawn in December '96.

Low-Frequency Dynamics probed with Coherent X-Rays

G. Grübel[1], D. Abernathy[1], T. Thurn-Albrecht[2], W. Steffen[2], A. Patkowski[2], G. Meier[2] and E.W. Fischer[2]

1 ESRF, Experiments Division
2 Max-Planck-Institut für Polymerforschung, Mainz, Germany

An intense coherent X-ray beam from ID10 (TROIKA) was used to study the low-frequency dynamics of colloidal palladium in glycerol by X-ray Photon Correlation Spectroscopy (XPCS). The measured relaxation rates were proportional to q^2 and viscosity as expected for a translational diffusion process. This experiment shows that XPCS can be performed in a wide time range (10^{-3} s to 100 s) and demonstrates a new opportunity for the study of low frequency dynamics in non-transparent systems.

X-ray Photon Correlation Spectroscopy (XPCS) can probe the dynamic properties of matter by analysing the temporal correlations among photons scattered by the material [1]. XPCS is sensitive to the low-frequency dynamics in a q-range from 1 x 10^{-3} Å^{-1} to several Å^{-1}, which is inaccessible to visible light and provides atomic resolution. It has been used in the time range from 1 s to 1000 s to study equilibrium fluctuations in Fe_3Al [2] and for studying Brownian motion of gold colloids [3]. We show in this experiment that XPCS can be performed in a wide time range (10^{-3} s to 100 s) by relaxing the bandpath of the coherent X-beam to the intrinsic bandwidth of an undulator harmonic (1.3% for the third harmonic of a 35 period undulator).

The experiment was performed at ID10 (TROIKA) of the European Synchrotron Radiation Facility (ESRF). The gap of the high-β undulator was tuned to provide photons of 8.2 keV energy at the peak of the third undulator harmonic. The transverse coherence length $\xi_t = \lambda R_S/2d_S$ of the X-ray beam was 52 μm (vertically) at R_S = 46 m from the source with a vertical size d_S = 67 μm. Primary slits at the 27 m point of the beamline were closed to 100 μm in order to provide a coherence length of 14 μm horizontally at the 46 m position. A flat water-cooled Si mirror (50 x 25 mm^2) located 44.2 m from the source was set to a critical energy just above 8.2 keV for rejection of higher harmonics and was used to deflect the beam horizontally out of the white undulator cone. A second Si mirror (150 x 40 mm^2) mounted on a piezoelectric bender was installed in vertical reflection geometry 0.76 m downstream of the first mirror in order to reduce the harmonic content to less than 5 x 10^{-3}. A laterally coherent X-ray beam was then produced by passing the X-rays through a 12 μm diameter pinhole aperture. The coherent flux was increased by focusing the beam vertically through the collimating pinhole until the vertical beam divergence matched the horizontal divergence giving a transverse coherence length of 14 μm in both directions. The integrated flux through the 12 μm pinhole was 10^9 photons/sec at 100 mA storage ring current. A set of guard slits of 100 μm size right in front of the sample removed scattering from the pinhole.

The longitudinal coherence length $\xi_l = \lambda(\lambda/\Delta\lambda)$ is determined by the bandwidth $\Delta\lambda/\lambda = 1/nN$ of the third (n=3) harmonic of the undulator with period N = 35. The measured bandwidth using a Si(111) analyser crystal was 1.3%. This corresponds to a longitudinal coherence length of 116 Å. In transmission geometry, the maximum path length difference (PLD) is given by $2h \sin\theta \tan\theta$, where h = 1 mm is the sample thickness. The requirement that PLD < ξ_l is satisfied up to scattering angles 2θ of 4.8 mrad corresponding to q = 2 x 10^{-2} Å^{-1}. This value extends considerably beyond the q range (q_{max} = 4 x 10^{-3} Å^{-1}) accessible with visible light. The low q limit is determined by the tails of the Fraunhofer diffraction of the main beam which in the present case is given by $q_{min} = 10^{-3}$ Å^{-1}.

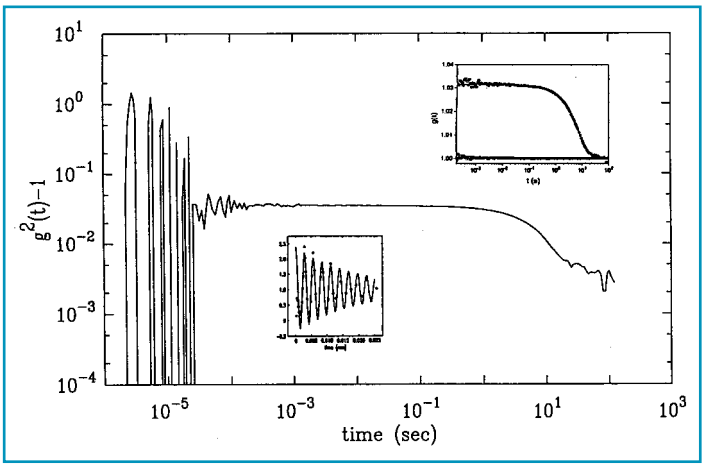

Fig. 1: Correlation function taken over 9 decades in time. The fast oscillation is quantified in the lower insert and corresponds to the velocity of the relativistic electron beam. The slow relaxation (upper insert) corresponds to the translational diffusion of the colloid.

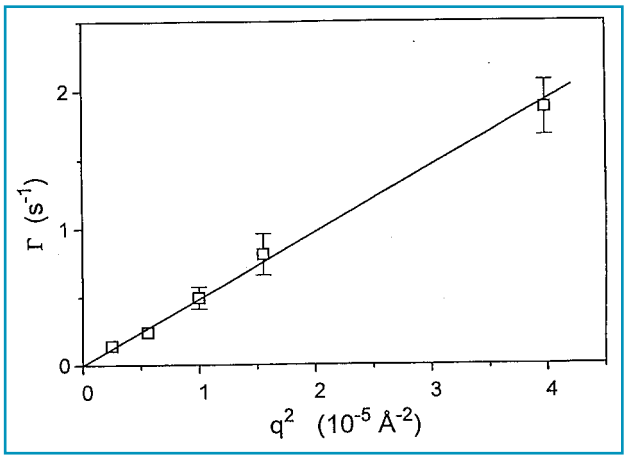

Fig. 2: Relaxation rates Γ determined from correlation functions taken at different q values. The linear relationship on q^2 confirms the diffusive nature of the observed process.

The sample was a solution of colloidal palladium in glycerol with a volume concentration of 0.3%. The colloid was coated with a stabilising agent and the sample was a completely opaque, black suspension. **Figure 1** shows a time correlation function covering 9 decades in time taken at q = 1.59 x 10^{-3} Å^{-1} at a temperature of 279 K. The oscillation visible at short times (t = 2.81 μs) is quantified in the lower insert and reflects the velocity of the relativistic electron beam. The slow relaxation at t > 1 s is quantified in the upper insert. It is well described by an exponential decay and corresponds to the translational diffusion of the palladium colloid. The correlation function for a diffusion process is given by g(q,t) = A(q)exp(-2Γt)+1, where the relaxation rate Γ = q^2D and D is the diffusion constant. The wave-vector dependence of the relaxation rates Γ are displayed in **Figure 2** and show the expected q^2 dependence over the whole q-range covered. The diffusion coefficient determined from the data is D = 5.1 x 10^{-12} cm^2 s at 279 K. For a translational diffusion process one expects D = kT/6πηR_h, where k is the Boltzmann constant, T the temperature, η the viscosity and R_h an apparent hydrodynamic radius of the diffusing particle. The temperature dependence of the relaxation rate Γ shows that the temperature dependence of the diffusion constant is in fact dominated by the viscosity of the glycerol solvent [4].

The experiment demonstrates that X-ray Photon Correlation Spectroscopy is uniquely suited to study slow relaxations at high scattering vector q with atomic resolution. Although the technique is still in its initial stage of development it has the potential of addressing important phenomena in disordered systems, such as critical fluctuations at an order-disorder transition, density fluctuations in liquids undergoing a glass transition, concentration fluctuations in polymer blends near phase separation or the short wavelength dynamics of fluids and colloids. ■

References:

[1] G. Grübel, J. Als-Nielsen, D. Abernathy, G. Vignaud, S. Brauer, G.B. Stephenson, S. G. J. Mochrie, M. Sutton, I. K. Robinson, R. Fleming, R. Pindak, S. Dierker, J. F. Legrand, ESRF Newsletter 20(1994)14;
G. Grübel, D. Abernathy, G. B. Stephenson, S. Brauer, I. McNulty, S. G. J. Mochrie, B. McClain, A. Sandy, M. Sutton, E. Dufresne, I. K. Robinson, R. Fleming, R. Pindak, S. Dierker, ESRF Newsletter 23 (1995) 14
[2] S. Brauer, G. B. Stephenson, M. Sutton, R. Brüning, E. Dufresne, S. G. J. Mochrie, G. Grübel, J. Als-Nielsen and D. Abernathy, Phys. Rev. Lett., 74, 2010 (1995)
[3] S. B. Dierker, R. Pindak, R. M. Fleming, I. K. Robinson, and L. Berman, Phys. Rev. Lett., 75, 449 (1995)
[4] T. Thurn-Albrecht, W. Steffen, A. Patkowski, G. Meier, E. W. Fischer, G. Grübel, D. Abernathy, to be published

Resonant Inelastic Scattering Using Circularly Polarised Soft X-Rays

L. Braicovich[1], N. B. Brookes[2], C. Dallera[1], G. Ghiringhelli[1] and J. B. Goedkoop[2]

1 Department of Physics, Politecnico di Milano, Italy
2 ESRF, Experiments Division

We describe the first experiments of circular dichroism in resonant soft X-ray inelastic scattering on disordered Fe-Co alloys.

It is well known that the core X-ray absorption in magnetic systems is polarisation dependent. If one uses circularly polarised radiation with the helicity parallel or antiparallel to the sample magnetisation the experiments show magnetic circular dichroism (MCD). This is particularly strong in 3d transition metals across the $L_{2,3}$ edges due to the dipole selection rules allowing direct access to the magnetic 3d states. In this connection a second generation experiment is to detect the spectral distribution of the emitted photons due to the core hole neutralisation instead of measuring only the absorption. In this case the experiment has to be regarded as a resonant inelastic scattering and it has been suggested that the scattering dichroism is related to the difference of the spin up and spin down populations of the occupied states of the system [1]. These experiments suffer from low intensity and therefore accurate work in this new field requires third generation synchrotrons.

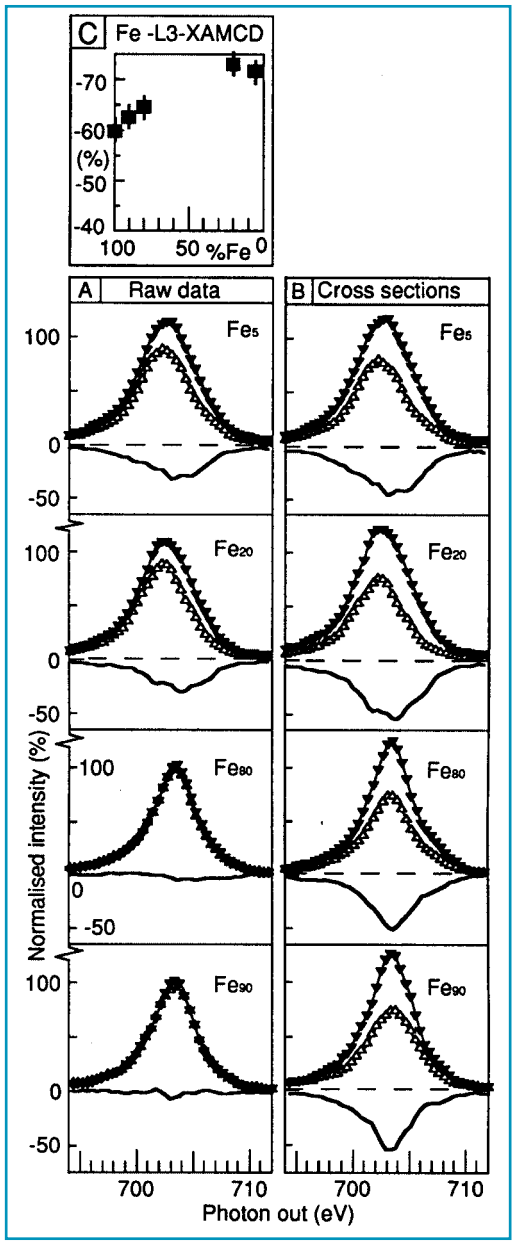

Fig. 1: A: measured scattering spectra from Fe-Co alloys films with Fe-L_3 excitation. B: the corresponding scattering cross sections. C: absorption MCD values at the Fe-L_3 edge for different Fe concentrations. All the values are corrected for polarisation and geometry. The open and closed triangles are for the two magnetisation directions and the lines are their difference.

The first experimental demonstration was made for Fe with white beam excitation at LURE [2] using the off-plane radiation from a bending magnet. Further experiments were performed with monochromatic excitation by Duda *et al.* [3](at SSRL) and by Hague *et al.* [4] (at LURE). At the ESRF a helical undulator beamline has been designed and installed at ID12 to make intense circularly polarised soft X-rays available. This article reports on the first measurements of scattering dichroism with monochromatic resonant excitation carried out at ID12B, the low energy branch of the beamline, with an apparatus that has been described in a previous issue of the ESRF Newsletter (n°24, June 1995). There we have already mentioned the non-resonant experiments using the whole undulator harmonic well above threshold.

As a specific example we will present data on disordered Fe-Co alloys. The samples were 600 Å thick films, prepared *ex situ* by coevaporation onto Si substrates and capped with 20 Å Au. We chose a 2.5 eV bandpass in the excitation channel and a 1.2 eV linewidth in the analyser. The counting rate integrated over the whole spectrum was above 3 counts/sec in the worst case. The circular polarisation rate was ~ 80 % at the energies used. The scattering spectra were measured by alternating every 5 minutes the magnetisation with a given sign of the light polarisation. During the measurements the field was kept on. Every two hours the phase of the undulator was changed and the spectra were measured with the opposite light polarisation. The samples were magnetised along the surface and the

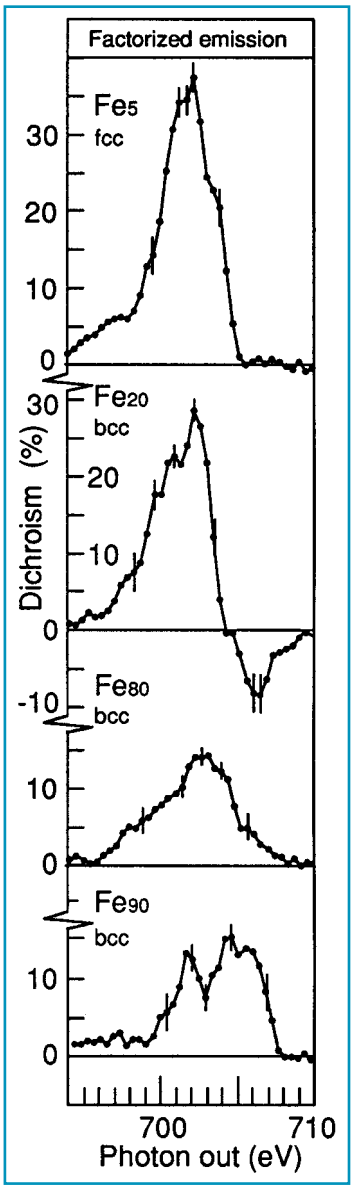

Fig. 2: The emission dichroism at Fe-L_3 edge obtained by factorising the scattering cross sections into an absorption and an emission cross section for different Fe concentrations. The error bars are given at selected points for readibility.

light was incident 20° from the surface, with emission normal to the surface. In the same set-up we also obtained absorption MCD from the sample drain current. In order to avoid artifacts due to magnetic stray fields a high voltage extracting electrode was facing the sample. We have studied a variety of compositions covering most of the interesting cases in Fe-Co magnetism and present here the scattering MCD of Fe in the alloys with L_3 excitation.

In **Figure 1a** we show the raw data and in **Figure 1b** the scattering cross-sections: these are obtained by considering that the incident radiation is absorbed on its way into the sample and that the outgoing radiation is self-absorbed. The absorption coefficient α is dichroic in the ingoing channel and not in the outgoing channel since the radiation was detected normal to the magnetic field. The relation between the scattering cross-section σ and the measured spectrum M from a sample of thickness T is (leaving out the self-absorption term to make the equation clearer):

$$\int_0^T \sigma^{\pm} \times \exp(-s \times \alpha_{in}^{\pm}) ds = (\sigma^{\pm}/\alpha_{in}^{\pm}) \times [1 - \exp(-T \times \alpha_{in}^{\pm})]$$

The scattering cross-sections of **Figure 1** have been rescaled to 100 % polarisation rate. We define the dichroism as the difference $(\sigma^+ - \sigma^-)$ with the normalisation $(\sigma^+_{max} - \sigma^-_{max}) / 2 = 100$. In panel C we show the absorption dichroism values that were measured. The scattering dichroism has the same sign as the absorption dichroism. However the scattering dichroism is smaller than the absorption dichroism, indicating that the effect of the outgoing channel has a kind of counter-effect. This is understandable since in an absorption experiment we look at the empty states, that are dominated by the minority spin. In a scattering experiment the radiation is first absorbed and then emitted, and in the emission process we look at the occupied states, that are dominated by the majority spin.

On the assumption that there is no interference between the ingoing and the outgoing channel, we can factorise the scattering cross-section into an absorption and an emission yield. This assumption is confirmed by a separate experiment on Co where we found that the L_3 scattering cross-section does not depend on the incident energy, ruling out temporal coherence effects of the type discussed by Ma [5]. Moreover these alloys are disordered systems and this washes out spatial coherence that would lead to *k*-selection rules. The emission dichroism obtained from the factorisation (**Figure 2**) should therefore be related to the spin-resolved density of states. These curves are in good qualitative agreement with electronic states calculations of Fe-Co alloys [6,7] and the trend of the emission dichroism in all samples follows the composition dependence of the Fe magnetic moment upon dilution [8].

In conclusion these experiments give information hardly obtainable with other methods, and can now be performed also on dilute systems exploiting third generation machines. ■

References

[1] *P. Strange, P. J. Durham, and B. L. Gyorffy, Phys. Rev. Lett. 67, 3590 (1991)*
[2] *C. F. Hague, J. M. Mariot, P. Strange, P. J. Durham, and B. L. Gyorffy, Phys. Rev. B 48, 3560 (1993)*
[3] *L.-C. Duda, J. Stohr, D. C. Mancini, A. Nilsson, N. Wassdahl, J. Nordgren, and M. G. Samant, Phys. Rev. B 50, 16758 (1994)*
[4] *C. F. Hague, J. M. Mariot, G. Y. Guo, K. Hricovini, and G. Krill, Phys. Rev. B 51, 1370 (1995)*
[5] *Y. Ma, Phys. Rev. B 49, 5799 (1994)*
[6] *K. Schwarz, P. Mohn, P. Blaha, and J. Kübler, J. of Phys. F: Met. Phys. 14, 2659 (1984)*
[7] *R. Richter and E. Eschrig, J. of Phys. F: Met. Phys. 18, 1813 (1988)*
[8] *S. Pizzini, A. Fontaine, E. Dartyge, C. Giorgetti, F. Baudelet, J. P. Kappler, F. Boher, and F. Giron, Phys. Rev. B 50, 3779 (1994)*

ACKNOWLEDGEMENTS

We would like to thank R. M. Jungblut and R. Coehoorn from Philips Eindhoven for preparing the samples. We would also like to thank M. Drescher and U. Heinzmann for providing the polarisation results prior to publication, and J. L. Hodeau for determining the structure of our samples by X-ray diffraction. This work was done under a INFM*/ESRF contract.

** Istituto Nazionale Fisica della Materia*

ULTRA SMALL-ANGLE X-RAY SCATTERING

O. DIAT[1], P. BÖSECKE[1], O. DHEZ[1], J. GORINI[1] AND J. LAMBARD[2]

1 ESRF, EXPERIMENTS DIVISION
2 CEA SACLAY, SCM, FRANCE

O. Diat and J. Lambard.

The performances of a high angular resolution small angle X-ray camera combined with an undulator source are presented in form of examples.

The structure of a collection of particles is characterised by the average position of the particles and by the interparticle spatial correlations. Small-angle scattering (SAS) is a scattering technique which allows structural information to be obtained over length scales between 1 to 100 nm depending on the radiation wavelength λ used (X-rays, neutron or visible light). In soft condensed matter, the use of hard X-rays (λ ≈ 1Å) allows to study the structure of all kind of materials to be studied although other radiations are sometimes more suitable (for contrast reasons for example). Polymers, colloidal systems in general, muscles, porous materials and so on are typically the physical or biological systems which are investigated using small-angle scattering techniques [1,2]. Also, the interactions which determine the thermodynamic stability of liquid systems have a signature in the small-angle scattering (for example, the limit at zero-angle of the scattered intensity versus the diffraction angle 2θ is proportional to the osmotic compressibility of the sample [3]). All this information is quantitatively analysed by studying the scattering intensity versus the scattering angle 2θ or the wave vector q defined as following: $q = 4\pi/\lambda \sin\theta$ and the corresponding length $d = 2\pi/q$.

Small-angle X-ray scattering (SAXS) experiments require, first, that the minimum scattering angle be detected (related to a good spatial or angular resolution) and second, that the signal to noise ratio be maximum. Therefore, the instrumentation must provide a well collimated and brilliant monochromatic beam at the sample position (with a minimum parasitic scattering around).

Two main types of SAXS cameras allow very low scattering angles to be achieved: either a pinhole camera using guard slits and a beamstop placed in front of the 1D- or 2D-detector [1,2,3] or a set of multiple-reflection crystals used as beam conditioners before and after the sample, e.g. a high angular resolution camera for ultra small-angle scattering (USAXS) [4-10]. The choice between both geometries depends on the specific needs for the experimental studies, i.e. high or low resolution Δθ/θ, one- or two-dimensional detection, static or time-resolved experiments, small or big beam cross-section. A common drawback is the parasitic diffuse and small-angle scattering arising from the direct beam through the optics and which superimposes on the scattering pattern produced by the sample.

During the commissioning of the High Brilliance beamline ID2 and during the two years of activity, a few short tests were carried out in order to determine the performance of a multiple crystal optics combined with a low divergence and high brilliance undulator source: the results were promising enough to persevere [10]. We present here a set of new data collected for the first time on ID2, the «High Brilliance beamline».

Figure 1 gives a schematic top view of the high angular resolution camera set-up on the beamline ID2. The crystal 1 (Si-111, 2 reflections in the vertical plane) belongs to the optics of the beamline. The crystals 2,3 (Si-220, 3 reflections in the horizontal plan) and crystal 4 (Si-111, 2 reflections in the vertical plane) are mounted on home-made goniometers with a step-resolution of 0.2 μrad around the θ axis (vertical for C2 and C3, horizontal for C4).

Fig. 1: High angular resolution camera set-up.

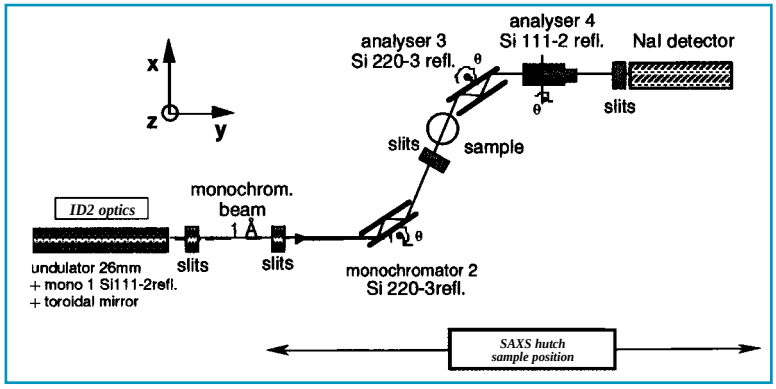

Figure 2 corresponds to the rocking curve of the crystal 2. The detection is carried out in the horizontal plane.

The full width at half maximum (~90 $Å^{-1}$) is the same on the two curves but the main difference is the large change in the slope of the scattering tails from about q^{-2} to q^{-3} visible on the Log-Log plot. In the first case (curve a) the vertical resolution is defined by vertical slits placed in front of the detector (~10 mrad acceptance) whereas in the second case (curve b) it is defined by the acceptance of the crystal 4 (~25 μrad). This means that the detected scattered signal, in the first case, contains a large contribution of the scattering out of the horizontal plane which is cut by the crystal 4 in the second case.

Fig. 2: Rocking curve of the crystal 2 with (a) only one analyser (crystal 3) and (b) with 2 crossed analysers (crystal 3 for the rock around the vertical q axis and crystal 4 at a fixed and optimised position).

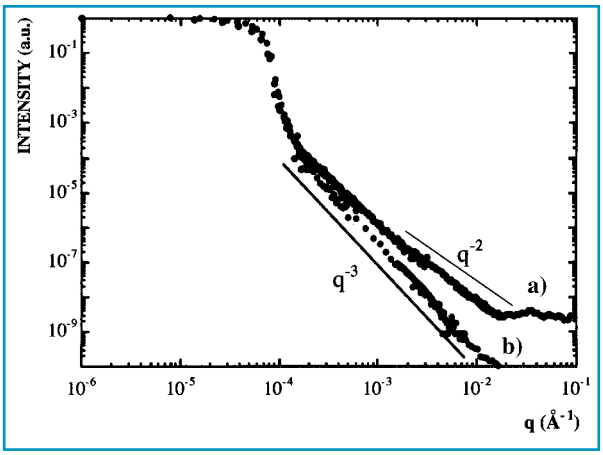

Fig. 3: Scattering profile of a solution of silica spheres (Stöber type, 6000 Å of diameter) in ethylene glycol solvent kindly provided by Rhône-Poulenc

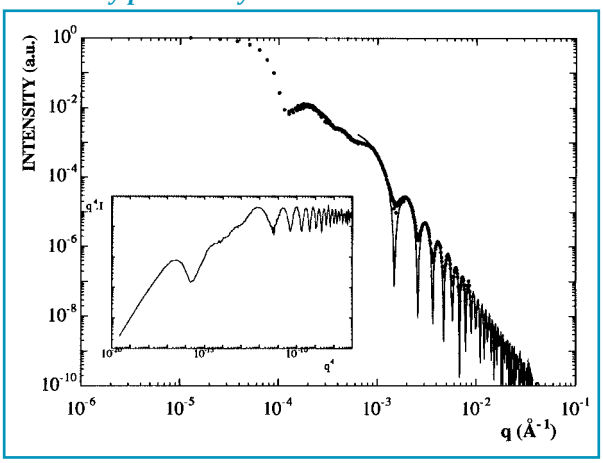

Fig. 4: Singular scattering around Bragg peak profiles.

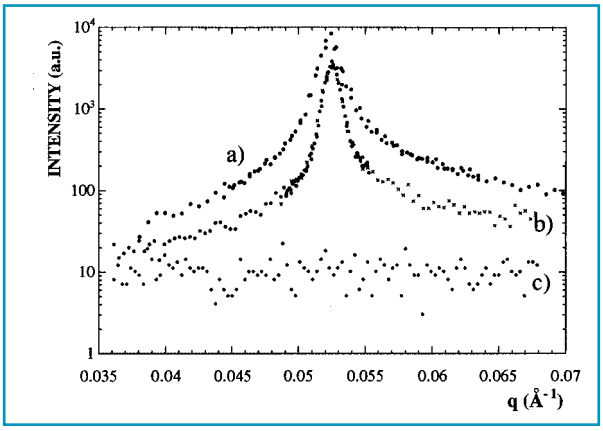

The use of both crossed analysers requires an important photon flux at the sample position which is available on ID2 (about 10^{10} ph/s) and allows the omission of some deconvolution operations in the case of only one analyser. Moreover the very low divergence of the undulator X-ray beam is comparable to the acceptance of the crystals, an advantage which increases the performances of such camera.

Figure 3 corresponds to the scattering profile of a solution of silica spheres. The intensity oscillations from the form factor of spheres (oscillations at large q vector) and the liquid order (at ultra-low q values) appear with a very high resolution. The raw data can be analysed without any deconvolution operations. The black line corresponds to a fit of the form factor for monodisperse spheres with a diameter of 6000 Å. The 3 decades of scattering angles were covered in 5 mn (1 second per point).

Figure 4 shows the possibility of analysing the singular scattering around Bragg peak profiles. The curve a) corresponds to a Bragg peak profile for a lamellar phase with a lamellae periodicity of 120 Å (phase of surfactant molecules) [12,13]. The curve b) corresponds to the profile of the same peak of the same lamellar phase but with some polymer between the surfactant bilayers. By analysing the decay of the Bragg peak tails we can get quantitative information on the elastic constants of the smectic crystals. This analysis is 100 times finer than the same one obtained from a standard 2D detector.

CONCLUSION

A few other tests have been performed on clays, large molecules like asphaltene in toluene (IFP), zeolites system [14], holograms in polymer matrix [11] and are very promising. A users' group has already used this set-up and could check the simple use of this camera which should be implemented on the beamline. ■

References

[1] *A. Guinier and G. Fournet, «Small-Angle Scattering of X-ray», John Wiley and Sons, New York (1955)*

[2] *K. C. Holmes, in «Small-Angle X-ray Scattering», O. Glatter and O. Kratky, editors. Academic Press, London (1982)*

[3] *At very small scattering angle, the system undergoes concentration fluctuations which are not independant since they are subjected to a constraint to keep the compressibility of the system unchanged*

[4] *J. Schelten and R. W. Hendricks, J. Appl. Cryst. 8 (1975) 421*

[5] *J. W. M. Du Mond Phys. Rev. Lett. 72 (1947) 512*

[6] *U. Bonse and M. Hart, Appl. Phys. Lett. 7 (1965) 238*

[7] *R. Pahl, U. Bonse, R. W. Pekala and J. H. Kinney, J. Appl. Cryst. 22 (1971) 771*

[8] *B. Chu, Y. Li and T. Gao, Rev. Sci. Instrum. 63 (1992) 4128*

[9] *J. Lambard, P. Lesieur and T. Zemb, J. Phys. I (France) 2 (1992) 1191*

[10] *R. Pahl, U. Bonse J. X-ray Sci. Tech., (1994)*

[11] *O. Diat, P. Bösecke, C. Ferrero, A. K. Freund, J. Lambard and R. Heintzmann, NIM A 356 (1995) 566*

[12] *Consequence of the Landau-Peierls effect - J. Als-Nielsen et al, Phys. Rev. B, 57, (1980), 312*

[13] *Test on samples from Ligoure et al, SC35 proposal « polymer induced phase separation in lyotropic smectics»*

[14] *T. M. P. Beelen, D. H. Bolt, I. P. De Moor, SC138 proposal, «USAXS on precursors of zeolites, molecular sieves and clays»*

ACKNOWLEDGEMENTS

We are greatly indebted to P. Wattecamps, J. Giovani and V. Rey Bakaikoa in providing quick solutions to many technical and computing problems. We are grateful to A. Paul and the Optics Group for providing a very good set of channel-cut crystals.

SINGLE CRYSTALS ABOVE ONE MEGABAR: PROGRESS REPORT

P. LOUBEYRE[1], R. LETOULLEC[1], D. HÄUSERMANN[2] AND M. HANFLAND[2]

1 DEP[T] OF «PHYSIQUE DES MILIEUX CONDENSÉS», UNIV. PIERRE ET MARIE CURIE, PARIS VI, FRANCE
2 ESRF, EXPERIMENTS DIVISION

X-ray diffraction studies of light materials (H_2, He, O_2, N_2, NH_3, H_2O...) at very high pressures are important from the point of view of the fundamental understanding of chemical bonding and the behaviour of their crystal and electronic structures under the extreme conditions found in planets and stars. As these studies require the highest possible X-ray brilliance to compensate for the high compressibility, low scattering power and tiny diffracting volume, major advances have been made at the ESRF. We summarise here the most recent results obtained on hydrogen and ice.

HYDROGEN

For hydrogen, structural information from tiny samples compressed between diamond anvils can so far only be obtained using single-crystal energy-dispersive diffraction (EDD), a technique originally developed at the NSLS to study this material. Conventional 4-circle geometry is replaced by rotation of the cell around two orthogonal axes only, while EDD spectra collected with white beam radiation at a fixed angle are scanned for reflections. This geometry allows faster measurements, and more importantly, it is better suited to diamond-anvil cell (DAC) studies of very light materials as it increases the ratio of sample signal to diamond background.

Accurate single crystal data on H_2 and D_2 have been obtained up to 120 GPa (1.2 Mbar) and this major breakthrough was made possible by combining this technique with two important developments: the growth of hydrogen single crystals in helium (see cover picture) to preserve the quality of the crystals in high compression conditions, and the development of large aperture DACs using X-ray transparent boron supports for the anvils.

The data collected so far are shown in **Figure 1** along with the early NSLS data of Mao et al. and the corresponding equation of state (EOS) refined by Hemley et al. No error bars are shown as they are smaller than the symbols. The solid line is a fit of a Vinet (EOS) to the ESRF data which revealed that hydrogen is more compressible than was thought from the older data. These measurements have shown that orientatio-nally disordered molecular hydrogen retains its hexagonal closed-packed structure to at least 120 GPa despite its high compressibility. They also revealed a decreasing c/a ratio, an indication that the gyrating molecules tend to orient perpendicular to the c-axis with increasing pressure; these are important results for narrowing down theoretical predictions of structural changes at higher pressures.

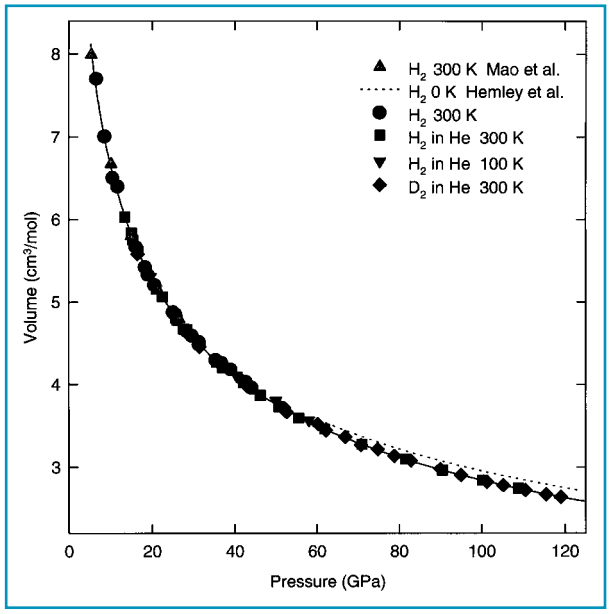

Fig. 1: Data and fitted equation of state of solid hydrogen and deuterium up to 120 GPa.

ICE VII

Cubic ice VII, the ambient temperature high pressure polymorph of ice has been studied up to 109 GPa as a powder [1] and up to 165 GPa as a single crystal. The powder measurements were carried out using vertically focused monochromatic radiation and image plates. A large enough number of ice VII reflections were followed up to the highest pressure to characterise the stress distribution within the sample and correct the measured pressure accordingly. The corrected compressibility data are shown in **Figure 2**. Unfortunately the diffracted intensity was not sufficient to follow the evolution of the hydrogen-only 111 reflection above 18 GPa. This important reflection is forbidden in the body centered cubic oxygen lattice, but makes fleeting appearances as the hydrogen atoms tend to preferentially localise on the body diagonal. When visible, it should thus give information on the state of proton ordering.

In order to bring out this very weak

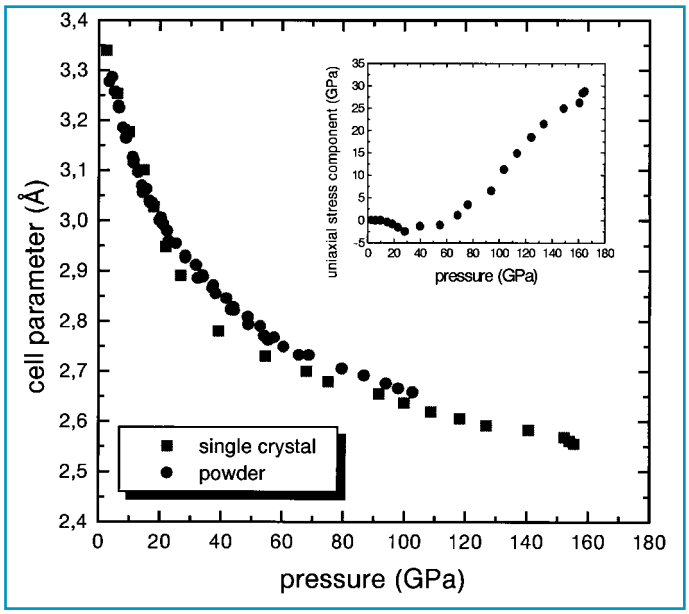

Fig. 2: Compressibility of cubic ice VII measured using powder and single crystal diffraction. The maximum pressure reached sets a new record in single crystal diffraction.

reflection, successful attempts were made at growing single crystals of ice VII and these led to a new record in single crystal diffraction under pressure: data were collected up to 165 GPa using the technique developed for the hydrogen work. These are also shown in **Figure 2** after correction for the measured uniaxial stress component (165 GPa has become 155 GPa). As their analysis is not yet completed, definitive conclusions cannot be drawn at this stage, but two comments can be made: (i) as expected the 111 reflection was indeed followed over the whole pressure range and it reveals different regimes of proton ordering, (ii) the disagreement between the powder and single crystal data (see **Figure 2**) is probably due to differences in stress conditions and sensitivity for the two techniques. For the powder, an «average» uniaxial stress component is assumed and found to increase, but for the single crystal measurements in which the stress conditions are better determined, the behaviour is different, as shown in the insert of **Figure 2**. A negative component possibly due to the compression of the «soft» gold liner used to protect the crystal in the rhenium gasket, dominates up to 30 GPa, whilst at higher pressures the stress behaviour ressembles that of the powder, at least qualitatively, as in the powder case we are dealing with average stress. Further measurements with different sample conditions are planned to better understand the different stress conditions.

It should be noted that in the case of the hydrogen measurements these problems are avoided by working in the quasi-hydrostatic conditions provided by the helium «cushion».

CONCLUSION

Recent single crystal results on very light materials have demonstrated the success of new high pressure diffraction techniques beyond 100 GPa. This is important for single crystal studies generally as it should help the development of this research field at very high pressures. ■

Reference

[1] P. Pruzan, E. Wolanin, J.C. Chervin, B. Canny, M. Gauthier, Department of «Physique des milieux condensés», Université Pierre et Marie Curie, Paris VI, France

VACANCIES AT THE ESRF ON 24 JUNE 1996

	Ref	Group	Position	Responsible
SCIENTISTS	2191	EXAFS	Beamline scientist (ID26)	J. Goulon
	PDID1 (2)	Anomalous Scatt	Postdoc (ID1) 2nd	M. Capitan
	PDID12A	XAS	Postdoc (ID12A)	J. Goulon
	PDID12B	EXAFS	Postdoc (ID12B)	J. Goulon
	PDID30	High Pressure	Postdoc (ID30)	D. Häusermann
	PDID30 (2)	High Pressure	Postdoc (ID30)	D. Häusermann
	PDBM5	Optics group	Postdoc (BM5)	A. Freund
CFR	CFR404	Theory	Thesis student	L. Farvacque
	CFR405	Radio Frequency	Thesis student	J. Jacob
ENGINEER	CDD/DP	Computing (MIS)	CDD Software Engineer	D. Porte
TECHNICIANS	2537	Experiments	Operator	C. Brändén / C. Kunz
ADMINIS.	CDD/MR	Central Services	Receptionist	M. Rodriguez

If you are interested in these positions, please send a letter with a copy of your CV mentioning the position you are applying for with its reference number to: Personnel Office, ESRF, BP 220, F-38043 Grenoble cedex.

X-RAY INELASTIC SCATTERING WITH NUCLEAR RESONANCE TECHNIQUES

A. I. CHUMAKOV[1], A. Q. R. BARON[1], R. RÜFFER[1], H. GRÜNSTEUDEL[1,2] AND H. F. GRÜNSTEUDEL[1]

1 **ESRF, EXPERIMENTS DIVISION**
2 **MEDIZINISCHE UNIVERSITÄT ZU LÜBECK, GERMANY**

A new technique to measure the energy distribution of X-ray inelastic scattering is developed. The well-defined transition energies in nuclei are used to analyse the energy of inelastically scattered radiation. The technique provides an easy way to study the density of vibrational states for a wide range of polymers and proteins.

The superior spectral density of radiation on the sample achieved at third generation synchrotron radiation sources allows one to establish new spectroscopies: nuclear and X-ray inelastic scattering with nuclear resonance techniques. The Nuclear Resonance beamline, ID18, [1] at the ESRF, is the first installation dedicated to nuclear resonance scattering.

The interaction of X-rays with nuclei occurs only within the very limited energy bandwidth (~0.01...0.1 μeV) near the nuclear transition, and the energy of this transition stays the same under any influence. This property makes nuclear transitions an excellent energy reference. We used this reference for the energy analysis in X-ray inelastic scattering experiments with samples that do not contain resonant nuclei [2].

EXPERIMENTAL SET-UP

The experimental set-up is shown in **Figure 1**. The X-ray beam is prepared by a high resolution monochromator (HRM) with 6.4 meV bandwidth. It has a compact 'nested' design [3], composed of Si (4 2 2) and Si (12 2 2) channel-cut crystals. The energy of the radiation is varied in steps of 1 meV in the range of ± 100 meV around the transition energy in ^{57}Fe (14413 eV). The typical flux on the sample is about 0.7×10^9 photons/s at 60 mA (16-bunch mode).

The energy of the radiation scattered by the sample is analysed using a resonance detector with a bandpass of 0.5 μeV. The detector consists of a large area (200 mm^2) fast avalanche photo diode (APD) [4] covered by a 10 μm foil of α-iron, 95% enriched in the resonant ^{57}Fe isotope. The resonant performance of the detector is determined by the process of elastic nuclear scattering in the foil. If the energy of the radiation coincides with the energy of the nuclear level, it excites the ^{57}Fe nuclei and is re-emitted forward with a time delay determined by the life time of the nuclear excited state (τ_0 = 141 ns). X-rays with other energies pass through the foil instantaneously. The delayed events are separated from the prompt pulse using fast electronics. The undesirable influence of inelastic nuclear absorption in iron is avoided in the detector design. The intensity of the delayed events is measured as function of the difference between the energy of the incident beam and the energy of the nuclear level. This measurement provides the probability of inelastic scattering as a function of energy transfer.

RESULTS

Energy spectra of X-ray inelastic scattering by water, polymethyl methacrylate, and gaseous Xe are shown in **Figure 2**. The presence of inelastic scattering is clearly seen, both in the considerable broadening and in the long tails of the spectra. The solid lines show the fit to the experimental data using a phenomenological approach (a), the density of states obtained in neutron studies (b), and a Doppler broadening model (c) [2].

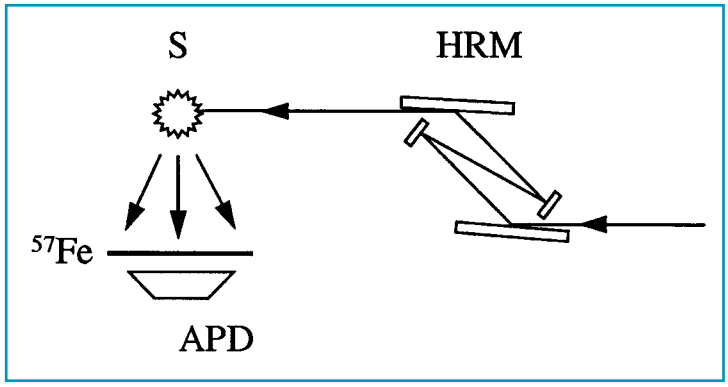

Fig. 1: Experimental set-up: HRM - compact high resolution monochromator with 6.4 meV bandpass, using Si(422) and Si(12 2 2) channel-cut crystals in a "nested" geometry; S - sample; ^{57}Fe - 10 μm foil of ^{57}Fe; APD - avalanche photo diode.

Nuclear resonant energy analysis of inelastic X-ray scattering offers a way to measure the energy distribution of the inelastic scattering, integrated over the momentum transfer. In this sense it is complementary to the conventional inelastic X-ray scattering technique with crystal optics analysis [5]. The new technique can be applied to measure a density of phonon states under the condition that q-dependence of the dynamic scattering function $S(q,\omega)$ is a common factor before the energy dependence of the scattering. This, for instance, is the case for many types of polymers [6] and proteins [7], thus a wide field of applications is anticipated. The first application of the new technique to study the vibrational dynamics in myoglobin with 4.4 meV energy resolution (upgraded high resolution monochromator at Nuclear Resonance beamline) was performed recently [8]. ■

References

[1] *R. Rüffer, A. I. Chumakov, Hyperfine Interaction, 97-98 589 (1996)*

[2] *A. I. Chumakov, A. Q. R. Baron, R. Rüffer, H. Grünsteudel, H. F. Grünsteudel and A. Meyer, Phys. Rev. Lett., 76 4258 (1996)*

[3] *T. Ishikawa, Y. Yoda, K. Izumi, C. K. Suzuki, X. W. Zhang, M. Ando and S. Kikuta, Rev. Sci. Instr., 63 1015 (1992); T. S. Toellner, T. Mooney, S. Shastri and E. E. Alp, SPIE Proceedings, 1740 218 (1992)*

[4] *A. Q. R. Baron and S. L. Ruby, Nucl. Instr. and Meth. A, 343 517 (1994)*

[5] *see e.g. F. Sette, G. Ruocco, M. Krisch, U. Bergmann, C. Masciovecchio, V. Mazzacurati, G. Signorelli and R. Verbeni, Phys. Rev. Lett. 75 850 (1995)*

[6] *B. Gabrys, J. S. Higgins, K. T. Ma and J. E. Roots, Macromolecules, 17 560 (1984)*

[7] *S. Cusak and W. Doster, Biophysical Journal, 58 243 (1990)*

[8] *K. Achterhold, C. Keppler, U. van Bürck, W. Potzel, P. Schindemann, E.-W. Knapp, B. Melchers, A. I. Chumakov, A. Q. R. Baron, R. Rüffer and F. Parak, European Biophysics Journal Letters, 24 (1996)*

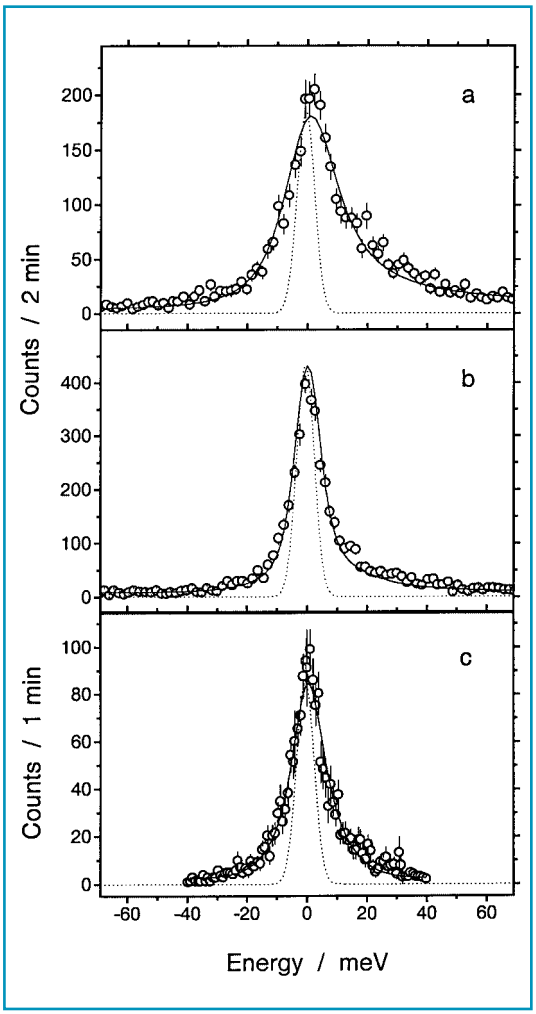

Fig. 2. Energy spectra of inelastic X-ray scattering by water (a); by polymethyl methacrylate (b), and by gaseous Xe (c). Solid lines show the fit to the experimental data. As comparison, the dashed lines show the instrumental function.

PHASE EQUILIBRIA OF CHARGED LAMELLAR PHASES

F. RICOUL[1], M. DUBOIS[1], A. VANDAIS[1], J-P. NOEL[1], T. ZEMB[1], M. LEFEVRE[2], D. PLUSQUELLEC[2] AND O. DIAT[3]

1 SERVICE DE CHIMIE MOLÉCULAIRE ET SERVICE DES MOLÉCULES MARQUÉES C.E.A. - SACLAY, FRANCE
2 ECOLE NATIONALE SUPÉRIEURE DE CHIMIE, RENNES, FRANCE
3 ESRF, EXPERIMENTS DIVISION

The goal of SAXS and osmotic pressure experiments is to determine the equation of state as well as the equilibrium phase diagrams of ternary systems made of two lipids. Coexisting lamellar phases are a sensitive tool to determine the relative importance of the different molecular forces involved. It will be shown how concentration gradient, labelled compounds and precise scattering experiments can be combined to quickly obtain the crucial zones in a ternary phase prism.

The amphiphilic molecules are constituted of two spatially distinct parts: a hydrophilic polar head and a hydrophobic tail. Due to this antagonist characteristic, these molecules aggregate (reversible process) in order to have a suitable environment around both parts; they are located at the boundary between polar and non-polar micro-domains. The variety of these molecules is very large, from industrial surfactants to lipidic proteins.

One type of this aggregation is the formation of bilayers of surfactants (or membranes) similar to the envelope of a biological cell. One way to understand the physical mechanism inside and between membranes is to make a simple system of bilayers with a well known model surfactant, to study the temperature and composition stability domains (i.e. phase behaviour at thermodynamic equilibrium), to incorporate one constituent of biological membranes step by step and then to study the change of physical properties.

An important component of all biological membranes involved in all recognition processes such as immunology reactions are glycolipids. These molecules belong to a family of molecules (class of glyco-conjugate) which have the unique property of having a large flexible hydrosoluble headgroup protruding from the membrane surface. To address this problem, we chose the ternary system: didodecyldimethyl ammonium bromide (DDAB) surfactant, 2-O-lauroylsaccharose (LS) [1] and water.

Interactions between surfactant bilayers are at the origin of swelling and non-swelling of lyotropic liquid crystalline phases in water (phases of surfactants). Determining boundaries of the phases coexistence as a function of salt and temperature is the oldest and most direct method to explore interactions between parallel bilayers versus distance. Four main interaction mechanisms exist between bilayers: 1) short-range decaying «hydration forces», 2) electrostatic screened forces, 3) steric undulation forces as repulsive forces are counterbalanced by 4) dispersion or van der Waals forces [2]. The best known synthetic surfactant type studied in this way is the double-tailed quaternary ammonium (DDAB) system [3].

Our aim is therefore to study in detail the effect of added surfactant with two large sugar-based headgroups (2-O-lauroylsucrose) compared to the effect obtained with other glycolipids and sugars. How does the presence of large sugar headgroups protruding from the bilayer surface influence the molecular force balance ?

To date some contradictory results have been published, force measurements between phospholipids/glangliosides bilayers showing an attractive adhesion force at the decompression (SFA technique) [4] and osmotic pressure data showing only repulsive steric interaction induced by the sugar headgroup [5,6].

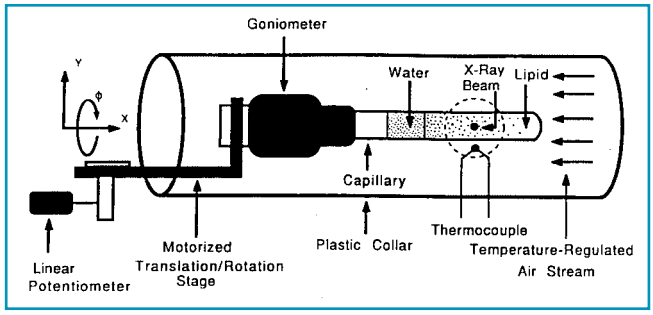

Fig. 1: Schematic diagram of the experimental arrangement for time-resolved X-ray diffraction from lyotropic gradient samples (from ref. [7]).

EXPERIMENTS

To address further that question in order to solve the ambiguity, the determination of ternary phase prisms is required as a first step (triangles of composition at different temperatures, as on Figure 4. Complete ternary phase prisms including glycolipids do not exist in literature due to the lack of availability of pure glycolipid (only available in mg quantities). The limits (low water as well as high water contents regime) of the single lamellar phase with mixed lipids have to be determined versus molar fractions and temperature. The lower concentration limit

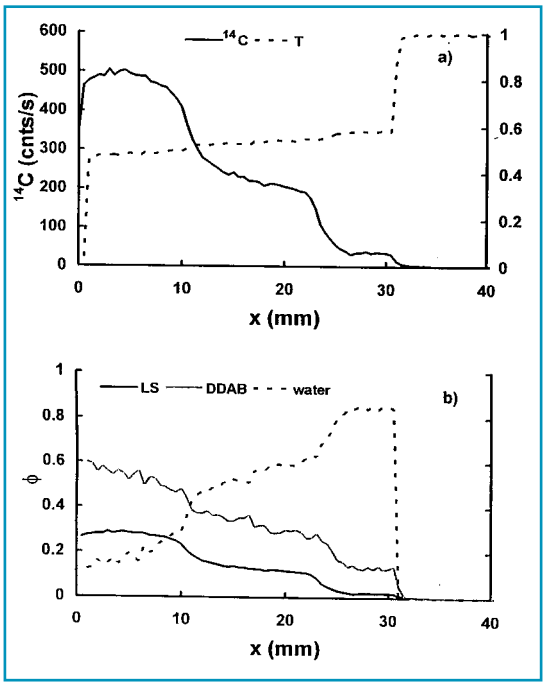

Fig. 2: In situ *analysis of the sample content along the capillary axis for a concentrated lamellar phase with an initial molar ratio LS/DDAB = 0.5 at one end of the glass tube, in contact with pure water. 2a) ^{14}C activity and the X-ray transmission measured on each point, 2b) sample composition deduced from 2a).*

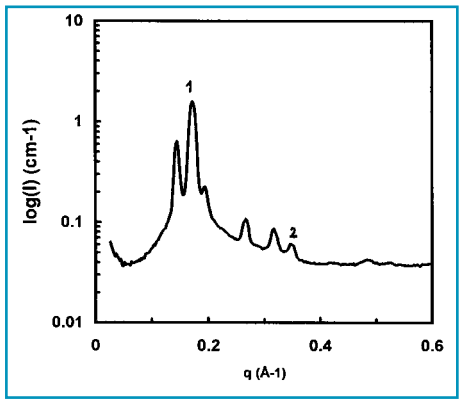

Fig. 3: Cubic and lamellar phase coexistence observed at the following composition: 20% of water, 24% DDAB and 56% LS. The first and second order of the lamellar Bragg peaks are labelled by (1) and (2).

involves an equilibrium between the maximum swollen lamellar phase and a very diluted aqueous phase: coexistence of lamellar phase, hydrated crystal and excess glycolipid. At this point of maximum dilution, osmotic pressure is zero: repulsive and attractive forces are balanced.

Scattering experiments have been carried out on the High Brilliance beamline (ID2) by extending the method of Caffrey to ternary systems [7]. The idea was to create a concentration gradient by diffusion in a capillary, at a constant temperature during a few hours incubation. A low concentration isotropic solution of glycolipids is put in contact with a concentrated lamellar phase. All the phases are present simultaneously in the capillary and may be studied at a constant temperature (double thermostat system, see **Figure 1**). The experiment has been performed on the water, DDAB and LS (2-O-lauroylsaccharose) ternary system (the sugar head is labelled with ^{14}C [7]). Samples have been prepared in 2 mm diameter borosilicate capillaries. An aliquot of a concentratred phase of a given composition was put in contact with a water solution in order to get a concentration gradient along the capillary axis. The beam size at sample has been set to 250 x 250 μm^2 allowing accurate mapping of the capillaries. Typical counting time to obtain a 512 x 512 frame was 60 seconds (optimisation between flux and exposure time in order to avoid radiation damage). Several capillaries at different temperatures have been exposed. The transmission of the beam has been recorded during the scan with an accuracy of the order of 1%.

In parallel, we made a determination of the composition of the sample along the axis with the same resolution by doing an auto-radiography of labelled glycolipid molecules with phosphor plates («molecular dynamics» image plate) in order to measure at any point of the capillary the concentration of the labelled molecule (which can be another membrane constituent). These two physical quantities give the concentration of the three components averaged over the illuminated point (see **Figure 2**). Here we used the high brilliance of the beam to increase spatial resolution of the analysis.

The determination of a ternary phase prism of a mixed system glycolipid/cationic DDAB/water in a large temperature range has been completed for the first time with a quantity of glycolipids as low as 400 mg in total. Up to now, the exploration of mixed systems phase diagrams had been limited to industrial surfactants easily available in large quantities.

The first set of experiments performed has allowed identification of three phases coexistence zones. **Figure 3** shows coexistence of a cubic and lamellar phase. In **Figure 4**, the three new coexistence

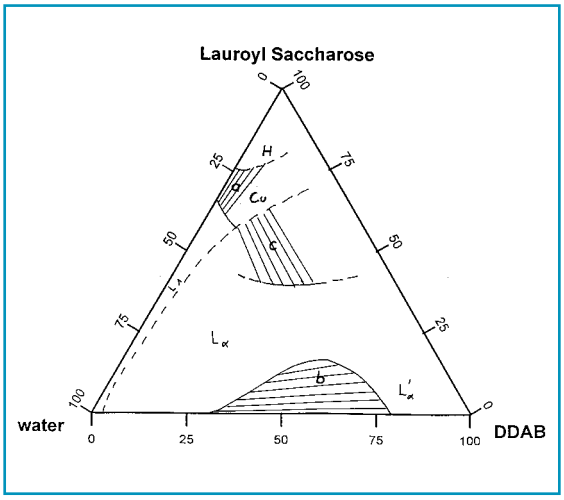

Fig. 4: First outline of the ternary phase diagram at T = 25 °C for the water/DDAB/LS system showing the three main coexistence regions : (a) micellar (L1) versus hexagonal (H) when the sample is rich in lauroylsaccharose, (b) collapsed (L'_{α}) versus swollen lamellar phase (L_{α}) when bilayers have a high surface charge and (c) lamellar (L_{α}) versus cubic (Cu) in the intermediate regime.

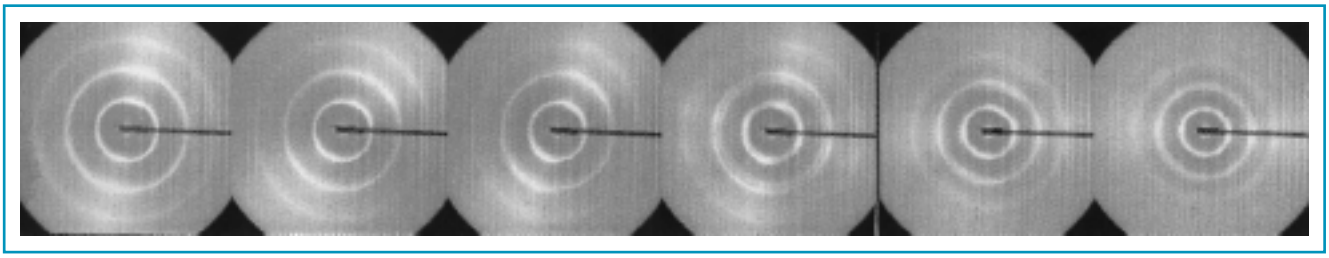

Fig.5: 2D scattering patterns illustrating stepwise swelling of the crystallites (multilayered vesicles) with lamellar symmetry structure (see especially the fourth from the left), along the water gradient, instead of the expected monotonic linear swelling.

regions are presented that we have shown in this experiment (a), (b), (c). Study of the periodicity in coexistence and measurement of the osmotic pressure of the plateau give a quantitative determination of the equation of state. Indeed, phase coexistence implies osmotic pressure identical in the two phases and so separation of the different interaction mechanisms.

An unexpected observation has been made due to the fine spatial resolution of the beam at the sample and is shown on Figure 5. Within a volume of 250 x 250 x 2000 μm^3 the swelling of the lamellar phase proceeds by finite steps instead of the expected continuous swelling.

The lamellar phase is present as a multilayered vesicular structure of very well-defined layering periodicity: during a typical counting time of 30 s, a very small number of crystallites are in the beam: on the recorded scattering pattern, sharp peaks are superimposed, implying well-ordered structures with a finite periodicity difference.

CONCLUSION

The feasibility of rapid efficient ternary phase diagrams on ID2 at the ESRF is demonstrated. As in metallurgy, phase diagram determination is the first necessary step in the comprehension of a mixed surfactant/lipid system. High brilliance, small beam size and 2D data collection on ID2 are necessary and will certainly allow exploration of other unknown complex phase equilibria by the community of soft condensed matter researchers. ■

References:

[1] C. Chauvin , K. Baczko and D. Plusquellec, J. Org. Chem.,58 (1993) 2291

[2] J. Israelachvili, «Intermolecular and surfaces forces», academic Press (1985)

[3] K. Fontell, A. Ceglie, B. Lindman and B. Ninham, Acta Chem. Scand., A40 (1986) 147; M. Dubois and Th. Zemb, Langmuir, 7 (1991)1352

[4] J. Wood, P. Luckham and R. Swart, Colloids and Surfaces A: Physicochem. Eng. Aspects, 77 (1993) 179

[5] T. McIntosh and S. Simon, Biochemistry, 33 (1994) 10477

[6] The osmotic pressure of solute-solvent system is the pressure due to the presence of solute molecules in the solvent, a quantity which is added to the pressure of the solvent alone under the same volume and temperature conditions

[7] M. Caffrey, Biophys. J., 55 (1989) 47

ACKNOWLEDGEMENTS

The authors would like to thank the Safety Group who gave us the authorisation to use a small quantity of ^{14}C labelled molecules in order to do this experiment, J. Gorini and P. Wattecamps for solving technical problems always at the last minute, M. Koscis for the supply of the gas-filled detector and also the Programming Group for making macros that we always asked for in a rush.

Mosaic Spread Measurements of Space-Grown and of Earth-Grown Protein Crystals

J.-L. Ferrer[1], J. Hirschler[1,2], M. Roth[1] and J. C. Fontecilla-Camps[1]

1 Institut de Biologie Structurale (IBS) - LCCP, Grenoble, France
2 Aérospatiale Espace et Défense, Les Mureaux, France

The CRG BM2 (D2AM) beamline, dedicated to Multiwavelength Anomalous Diffraction experiments of crystals of biological macromolecules, has been used for the first time to measure the mosaicity of protein crystals. These measurements consist of a detailed analysis of the rocking curves of selected reflections. They were performed on crystals grown under microgravity conditions as well as on crystals grown in the laboratory. This permits an unambiguous judgment of the quality of protein crystal obtained from different growth environments.

Developments in X-ray generation, data acquisition and computing techniques have significantly advanced protein crystallography in the last few years. One domain that has not followed this general trend is protein crystallisation, which is thus increasingly becoming the limiting factor in the successful determination of protein structures. As there is no *a priori* knowledge of the crystallisation conditions of newly obtained proteins, systematic screening of a large number of parameters is needed to find their respective crystallisation conditions. There is no guarantee yet that this tedious process will yield crystals at all, nor that the crystals obtained will be of sufficient quality for subsequent X-ray experiments.

A new parameter is introduced with crystallisation under microgravity conditions (either on unmanned re-entry satellites, manned space stations or NASA space shuttle). This new technique has received widespread attention as a result of reports indicating improved protein crystal quality in this environment compared to crystallisation at unit gravity. These potential improvements are generally attributed to the lack of convective flow around the growing crystals in the absence of gravity. However, the important question remains of how to unambiguously quantify the crystal quality of space-grown crystals. Only such a quantification will allow us to determine how much improvement the parameter microgravity really brings about in the crystallisation process. Maximum diffraction limits and signal-to-noise ratios of the data, which mainly depend on the diffracted intensity, are the most commonly used criteria. The crystal mosaicity is another important criterion, which gives the angular dispersion of the different small perfect crystal blocks of which an imperfect crystal is made. The smaller the mosaicity, the narrower the profiles of the measured reflections and the higher they will stand out from background noise. Consequently, this gives an unbiased measurement of the intrinsic crystal properties, allowing judgement of the actual contribution of microgravity-based effects to crystal quality improvements. Unfortunately, mosaicity measurements have been hindered by poor beam characteristics of classical X-ray sources (low intensity and large beam divergence) in the past. The problem has been overcome with the availability of synchrotron radiation beam characteristics, allowing protein crystal mosaic spread measurements using custom-made instrumentation [1, 2].

Here, we present preliminary protein crystal mosaic spread measurements, recorded using standard protein crystal data collection equipment on beamline D2AM. These measurements were performed on crystals of turkey egg white lysozyme (TEWL), grown under microgravity conditions on board NASA space shuttle mission STS-72 in January 1996 as well as on corresponding earth-grown TEWL crystals. TEWL is a small protein of 14.2 kDa molecular weight, which we have already used as a model system for contamination and kinetic growth studies [3]. The earth-grown crystals were obtained by the vapor-diffusion method according to published crystallisation conditions [3]. This method takes advantage of the equilibration of a droplet with a low precipitant concentration against a reservoir solution of high precipitant concentration through the gas phase. Crystallisation is brought about by the slow increase of the protein concentration in the droplet. The crystallisation conditions for the space-grown crystals using the Vapor Diffusion Apparatus (VDA, [4]) were derived from those of the earth-grown crystals. The VDA consists of a syringe, whose double barrels are filled with 15 μl TEWL solution and with 15 μl precipitant solution. Once microgravity conditions are reached, the VDA is activated by advancing the double piston, which lets the two solutions come into contact and form one single droplet. This droplet slowly equilibrates against the surrounding reservoir, which consists of 1.4 ml precipitant solution absorbed by a porous plastic. When entering gravity conditions, the obtained crystals are retracted into the syringes by pulling back the double pistons. After the space shuttle

landed, the crystals were recovered, transferred to the Institute of Structural Biology and mounted in standard glass capillaries of 0.7 mm diameter.

MEASUREMENTS

When performing oscillation camera data collection, a reflection can be observed over a more or less wide oscillation range. This reflection range depends on the mosaicity of the crystal, but it can be increased by other effects, such as beam divergence and wavelength spread of the X-ray source. This can be modelled considering that each reciprocal-lattice point is represented by a spherical volume element of radius ε. According to the model, and for reflections which are not too close to the blind region ($4\xi^2$-d^{*4} large enough, see below), the reflecting range φ_r of a fully recorded reflection is expressed as [5]:

$$\varphi_r \approx L d^* [(\gamma(\alpha) + \eta) \cos\theta + (\delta\lambda/\lambda) \sin\theta] \quad (1)$$

where $d^*=\lambda/d$ (λ is the average wavelength of the X ray beam), ξ is the projection of d* perpendicular to the rotation axis y, L is the Lorentz factor, $\delta\lambda/\lambda$ is the spectral dispersion and η is the mosaic spread. In this expression, θ is the Bragg angle of the considered reflection and γ the mean divergence in the plane defined by the direct and the diffracted beams ($\gamma = [(\gamma_x \sin\alpha)^2+(\gamma_y \cos\alpha)^2]^{1/2}$, with γ_x and γ_y respectively the beam divergence in the x and y directions and $\tan\alpha = x/y$). Coordinates of the reflection are given in the laboratory reference frame where y is the rotation axis, horizontal and perpendicular to the direct beam, z is the horizontal axis parallel to the direct beam and x the vertical axis. When the reflection is in the vertical plane with respect to the direct beam, (1) becomes:

$$\varphi_r \approx \gamma + \eta + (\delta\lambda/\lambda) \tan\theta \quad (2)$$

The measurements were performed on the D2AM beamline. This beamline is built on a bending magnet source with a 19.5 keV critical energy and a 0.16 mrad vertical divergence at 1 Å wavelength, measured at the full width at half maximum (fwhm). The optics consists of a two-crystal monochromator placed between two grazing angle mirrors. Reflection and diffraction are in the vertical plane [6]. The first mirror collimates the beam parallel in the vertical plane on the first crystal, which is flat. The vertical divergence of the incident beam is thus nearly zero. The second crystal is sagitally bent in order to perform a horizontal focusing with a 3:1 demagnification. The second mirror performs the vertical focusing on the sample. At optimal incidence, the mirrors perform together a harmonics rejection of 10^{-4}. The focused beam on the sample is 0.3 mm in diameter, with a 0.48 mrad maximum vertical divergence (fwhm) and 9 mrad maximum horizontal divergence. The intensity of the full beam is about 10^{11} ph/sec at 1 Å wavelength.

The beamline D2AM has been designed specifically to take advantage of the anomalous signal, with an energy resolution improved by the collimation of the first mirror. The resulting energy resolution $\delta\lambda/\lambda$ is estimated to be as good as ~10^{-4}. This means that for our mosaicity measurements the term proportional to $\delta\lambda/\lambda$ in relation (2) can be neglected in comparison to the vertical divergence of the incident beam on the crystal for a reflection range >> 1 mdeg and at low resolution (d > 5 Å).

The diffractometer for biological macromolecular crystallography was

Fig. 1: Three representative reflection profiles of an earth-grown TEWL crystal chosen in the vertical plane of diffraction (rotation axis is horizontal and perpendicular to the beam) and at approx. 5 Å resolution. The respective full width at half height (fwhm) of the gaussian fits of these profiles (represented by the thin solid line for the most intense profile) are 31.4 mdeg (full line), 53.5 mdeg (dashed line) and 52.6 mdeg (dotted line) respectively.

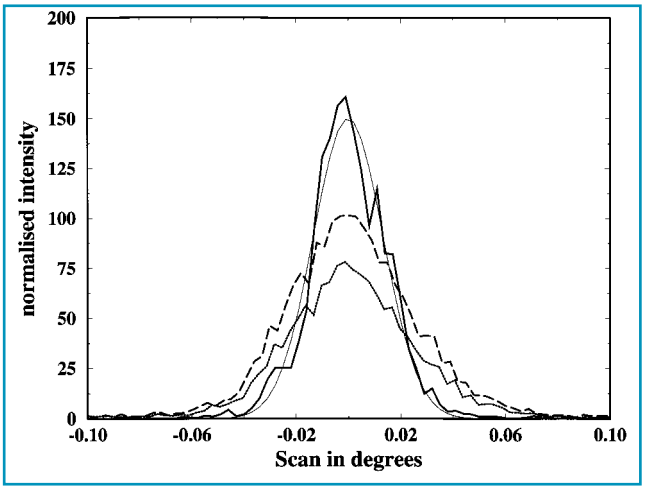

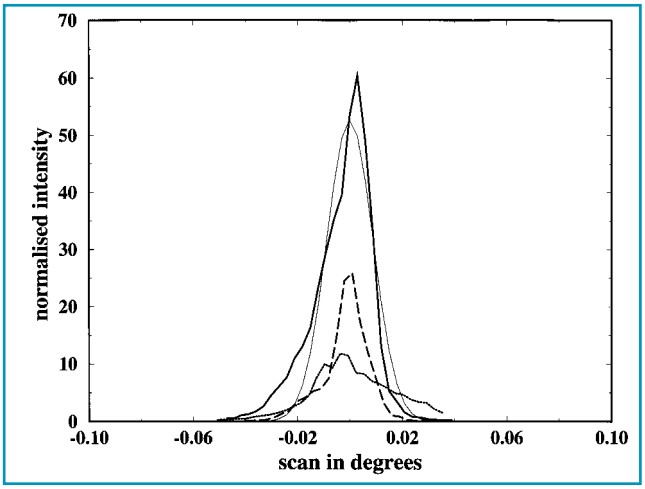

Fig. 2: Three reflection profiles of a microgravity-grown crystal. Their fwhm are 20.6 mdeg (strong solid line, thin line representing its gaussian fit), 14.4 mdeg (dashed line) and 35.8 mdeg (dotted line), respectively. The comparison with the profiles of the earth-grown crystal shows that these profiles are much smoother, containing virtually no shoulders, and that they have a smaller fwhm.

also especially designed for Multiwavelength Anomalous Diffraction (MAD) data collection [7]. It features a fully motorised goniometer head with an x,y,z translation stage allowing remote centering of the crystal, and an arc+spindle rotation stage. The rotation axis for data collection is horizontal and the rotation range is currently as large as 250 deg, with 10000 steps/deg. Data is collected on an ESRF type CCD detector with a 16-bit, 1242 x 1152 pixels CCD camera. In a classical MAD experiment, the data are collected with typically 0.5° crystal rotation and few seconds exposure time per frame.

RESULTS AND DISCUSSION

Data processing for the mosaicity analysis was performed by the program MOSAICITY**.** This program has been developed specifically for this experiment but is now available as a general tool for crystal quality evaluation prior to standard data collection. A detailed knowledge of the mosaic spread also improves the data processing step.

We have carried out a preliminary evaluation of the crystals. Some reflection profiles are presented below. The profiles are not corrected for Lorentz broadening and other contributions previously described. However, in order to minimise the γ and the $\delta\lambda/\lambda$ terms in (2), only those reflections located in the vertical plane including the incident beam and those at low resolution (> 5 Å) are considered for the moment.

Data on the earth-grown crystal were first collected at λ = 0.98 Å, with oscillation ranges of 0.5 deg for the indexing of the reflections and then with an oscillation of 0.003 deg for the rocking curve analyses. **Figure 1** shows three representative reflection profiles of this crystal. The respective fwhm of the gaussian fit of these profiles are 31.4 mdeg (full line), 53.5 mdeg (dashed line) and 52.6 mdeg (dotted line). They show rather rugged profiles displaying several shoulders. Comparison of the positions of the shoulders of the three curves (recorded at different times in the same data collection process) shows that their positions are roughly coincident. This suggests that they do not result from accidental fluctuations in the experimental set-up, but that they are intrinsic features of the crystal. Corrections for Lorentz factors, beam divergence and energy resolution to be implemented may further improve the coincidence of these shoulders. Further fitting analysis will show if the peaks containing shoulders can be systematically decomposed into several minor peaks. Each minor peak may then be interpreted as arising from a single crystallite of the mosaic crystal. The number of peaks would then correspond to the number of crystallites detected under the experimental resolution used.

Figure 2 shows three reflection profiles of a microgravity-grown crystal, which were obtained as described before. Comparison of these profiles to those of the earth-grown crystal shows that the profiles obtained here are smooth, containing no shoulders. According to the reasoning presented above, future fitting may show that these peaks cannot be further decomposed into a combination of peaks. If so, it would indicate that the microgravity-grown crystal does not display discrete crystallites, but that it is made up of a single crystallite with a mosaicity smaller than that detectable here.

The fwhm of the microgravity-grown crystal are 20.6 mdeg (full line), 14.4 mdeg (dashed line) and 35.8 mdeg (dotted line). They are hence smaller than those of the earth-grown crystal. This suggests a smaller angular dispersion of the crystallites in the microgravity-grown crystal than in the earth-grown crystal. Further analysis will permit the differences found here to be better characterised, especially with regard to corrections for Lorentz factors and detector distortion. It should be noted, however, that the observations presented here apply to TEWL, and that corresponding results on other protein crystals may be different.

The difference in crystal quality between microgravity- and earth-grown crystals is generally attributed to the lack of convective flow in the former. Solutal flow around growing protein crystals has been shown to slow down their growth in the laboratory [8]. Further analysis of our data will determine whether the decreased flow in microgravity conditions can be correlated to a smaller TEWL crystal mosaic spread.

Our results also show that mosaicity measurements of crystals with mosaic spreads as low as 15 mdeg can easily be carried out on the D2AM beamline in its standard configuration. ■

References

[1] E. H. Snell, S. Weissgerber, J. R. Helliwell, E. Weckert, K. Hoelzer and K. Schroer, Acta Cryst. D51 (1995) 1099-1102

[2] R. Fourme, A. Ducruix, M. Riess-Kautt and B. Chapelle, J. Synchr. Rad. 2 (1995) 136

[3] J. Hirschler and J. C. Fontecilla-Camps, J. Crystal Growth, in press

[4] L. J. DeLucas et al., J. Crystal Growth 76 (1986) 681-693

[5] T. J. Greenhough and J. R. Helliwell, J. Appl. Cryst. 15 (1982) 338-351

[6] J. P. Simon, E. Geissler, A. M. Hecht, F. Bley, F. Livet, M. Roth, J.-L. Ferrer, E. Fanchon, C. Cohen-Addad and J.-C.Thierry, Rev. Sci. Instrum. 63 (1992) 1051

[7] E. Fanchon, J-L. Ferrer, R. Kahn, C. Berthet and M. Roth, ESRF Newsletter 24 (1995) 6

[8] M. Pusey, W. Witherow and R. Naumann, J. Crystal Growth 90 (1988) 105-111

ACKNOWLEDGEMENTS

We thank Dr. Larry DeLucas and Dr. Karen Moore of the Center for Macromolecular Crystallography at the University of Alabama at Birmingham/USA for providing the opportunity to carry out the microgravity crystallisation experiments on NASA space shuttle mission STS-72. Support by the European Space Agency is gratefully acknowledged via the RADIUS on Biotechnology.

CAPILLARY OPTICS

P. ENGSTRÖM[1], A. RINDBY[2] AND L. VINCZE[3]

1 ESRF, EXPERIMENTS DIVISION
2 DEPT OF PHYSICS, CHALMERS UNIVERSITY OF TECHNOLOGY, SWEDEN
3 DEPT OF CHEMISTRY, UIA, ANTWERP, BELGIUM

Capillary optics is one of the fastest growing X-ray optical technologies because of its superior capacity of generating high flux density beam in the µm - and sub µm range. Due to its broad band characteristic, non-imaging properties and simplicity, it is a perfect optical device for microbeam X-ray fluorescence and X-ray scanning microscopy.

At the ESRF, conical and ellipsoidal capillaries have been used as «post» focusing concentrators at ID13 generating flux densities of the order of 10^{10} photons/μm^2/s at a bandwidth of 2×10^{-4}. With these beam characteristics (probably the most powerful microbeam in the world right now) a number of users' experiments, within the fields of wide-angle scattering [1], micro X-ray diffraction and simultaneous micro X-ray fluorescence/micro X-ray diffraction [2], have been carried out at a microscopic level.

Although capillary optics have developed very rapidly during the last 5 years, there are still controversies and unsolved problems concerning the actual refraction and reflection of the radiation inside the capillary. Different models for the capillary surface roughness have been proposed, however real experimental data is scarce due to the difficulties of making direct measurements on the inner surfaces of μm-sized capillary. However, by measuring the angular distribution out from the capillary, the surface roughness can be estimated in an indirect way. Especially when the capillary is deliberately misaligned the surface roughness will be critical to the precise shape of the 2D angular distribution. In the experiment carried out at the optical beam and at ID13 the angular distribution from different capillaries has been carefully measured and compared with ray-tracing calculation simulating the actual shape of real capillaries, which is demonstrated below.

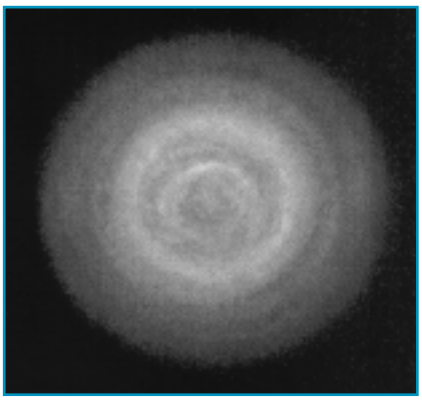

Fig. 1: Angular distribution of radiation coming out from a "real" well-aligned capillary. The image was recorded by a CCD camera a few cm away from the opening of the capillary.

Next to obvious parameters such as the capillary shape and dimensions (start and end diameters, length), a number of other factors influence the performance of capillary devices. These include the material of which the capillary is made (e.g., borosilicate glass or lead glass), the surface roughness of the reflecting surface and the deviation in shape that real devices assume in comparison to the 'ideal' straight, conical or ellipsoidal shapes. Next to that, the size, divergence and distance of the X-ray source and the energy or energy distribution of the photons that enter the capillary also strongly influence the performance of a capillary device with a given set of physical characteristics.

Because so many factors may have an influence on the capillary performance, it is hard to quantitatively assess the significance of each individual factor by interpretation of experimental results only. This problem is augmented by the fact that the manufacture of capillary optics is still very much an art rather than a well-controlled technique, making it difficult to produce a series of capillaries where one parameter is systematically varied. The need to gain insight into the relative importance of the various above-mentioned factors has prompted the development of a detailed ray-tracing code [3,4], which is able to simulate the beam-forming properties of realistic capillary devices assuming various experimental conditions.

The code uses the Monte Carlo technique to model the propagation of X-rays through the glass tube as they undergo multiple reflections on the capillary walls. Since the capillaries in the simulation are treated as truly three-dimensional devices having numerically defined shapes, the only restriction on the modelled shape is its assumed circular cross-section in the plane perpendicular to the capillary axis. This allows overall distortions of the capillary shape, such as bending of the capillary axis, to be included in the model. Also, the composition of the capillary material as well as the roughness of the reflecting surface can be freely chosen. The implemented surface roughness model describes both the attenuation of the specular reflectivity and the effects of diffuse scattering by the rough surface.

An additional feature of the program is that the possible transmission of photons through the capillary wall is also taken into account. As

demonstrated by the example above, the code can reasonably predict the rather complex beam profiles produced by capillary optics which have been observed during recent experiments at ESRF bending magnet (BM5) and undulator (ID13) sources.

When applying a real monochromatic point source (like ID13 at the ESRF) the individual rings representing different reflection orders will become visible and can therefore be studied directly on the screen when the capillary is misaligned. Thus, it is possible to measure the reflectivity versus angle of incident at different positions within the capillary without actually cutting it. This will be very important for testing different models for surface roughness and also to determine the impact of different types of fabrication techniques and treatments used to improve the surface qualities. **Figures 1 and 2** show a nice symmetric angular distribution which is in reasonable agreement with the simulated distribution, for a well-aligned capillary. **Figures 3 and 4** show a misaligned capillary.

Any experimental characterisation of capillary devices has to be performed in parallel with some kind of ray-tracing calculation. It is absolutely vital that the ray-tracing algorithm used is realistic and that it can be applied to «real» capillary shapes. The code developed by L.Vincze at the University of Antwerp is probably the most comprehensive model of capillary refraction right now and has proven to be able to reconstruct realistic distributions from «real» capillary shapes. ■

References

[1] P. Engström, C. Riekel, H. Chancy. Experiments with Glass Capillary Optics on the Microfocus Beamline. ESRF Newsletter 24, 8-9, (June 1995)

[2] A. Rindby, P. Engström, J. Osan, S. Török, K. Janssens. Simultaneous μ-fluorescens and μ-diffraction of fly-ash particles (in manuscript)

[3] L. Vincze, K. Janssens, F. Adams and A. Rindby. Detailed Ray-Tracing Code for Capillary Optics. X-Ray Spectrometry, Vol. 24, 27-37 (1995)

[4] L. Vincze. Ph.D. Thesis, University of Antwerp, Belgium (1995)

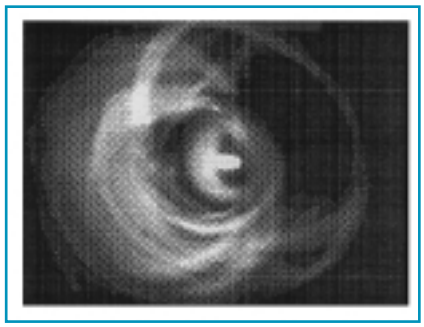

Fig. 3: Angular distribution of radiation coming out from "real" misaligned capillary. The image was recorded by a CCD camera a few cm away from the 8 μm opening of the capillary.

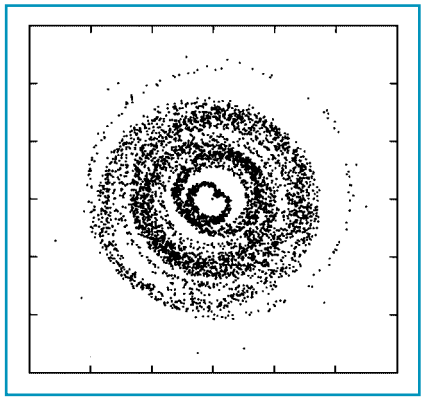

Fig. 4: A simulated spatial intensity distribution at a few cm distance from a misaligned capillary. The original symmetric bands, which are obtained in case of perfect alignment, now appear as asymmetric halos around the central spot.

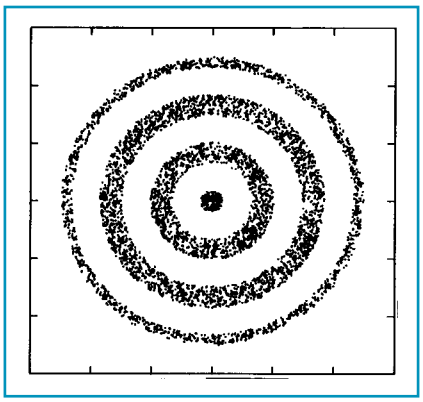

Fig. 2a: A simulated spatial intensity distribution from a perfect aligned «ideal» capillary. The symmetric rings representing different reflection modes appear as asymmetric halos around the central spot.

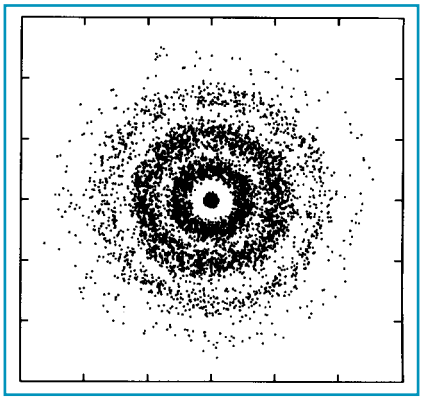

Fig. 2b: As 2a but a surface roughness of 30 Å introduced.

JITTER-FREE ACCUMULATING STREAK CAMERA WITH 100 FEMTO-SECOND TIME RESOLUTION

G. MOUROU[1], G. NAYLOR[2], K. SCHEIDT[2] AND M. WULFF[3]

1 CENTRE FOR ULTRAFAST OPTICAL SCIENCE, MICHIGAN, USA
2 ESRF, MACHINE DIVISION
3 ESRF, EXPERIMENTS DIVISION

The scientific interest in ultra-short X-ray pulses corresponds to specifications that a circular machine like the ESRF is not able to meet. However, a new type of ultra-fast detector coupled with an equally fast and powerful laser offers the possibility of attaining sub-pico-second time resolution whilst using the 150 ps ESRF bunch length. The original idea came from G. Mourou and his team at the Centre for Ultrafast Optical Science (CUOS) in Michigan, USA. A collaboration project has started between CUOS and the ESRF to develop and construct such a 100 femto-second streak camera detector system over the next three years. Such a system would break completely new ground in time-resolved X-ray scattering experiments.

One of the conclusions of the ICFA workshop on 4th Generation Light Sources was the increasing interest of the scientific community in ultra-short pulses for dynamic studies [1,2]. However, third generation light sources experience a limitation in the production of such short pulses. At the ESRF, the flexibility of the storage ring lattice has enabled studies with the machine operating in a quasi-isochronous mode and at below nominal energy in order to reduce the electron bunch length. These efforts have shown that a sub ps range will not be accessible due to intrinsic limitations of a circular machine [3].

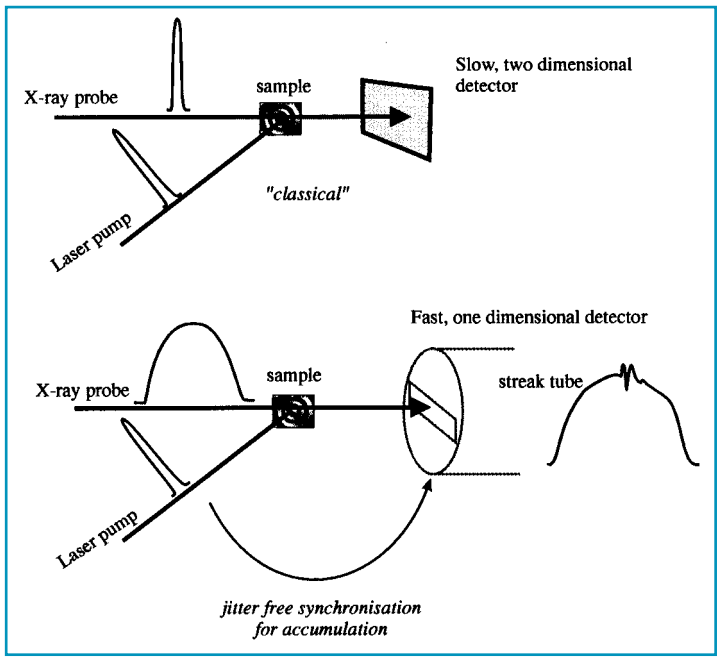

Fig. 1: Experimental arrangements for time-resolved X-rays measurements.

Linac-driven free-electron lasers offer the potential to achieve this ultra-short characteristic of high energy, high brilliance X-ray pulses. However, their research and development program is yet to start and such a 4th generation light source would not come into routine user operation until about 20 years from now.

Fortunately, exciting developments in ultra-fast laser and detector technology have taken place over the last 20 years. Their application, combined with the high brilliance ESRF X-ray source operating in single bunch or hybrid filling mode, will make it possible to carry out ultra-fast dynamic experiments with sub-ps time resolution using an adapted measurement concept [4, 5].

NEW CONCEPT

The «classical» concept of experiments for time-resolved scattering research would use an ultra-short X-ray *probing* pulse together with an optical laser *pumping* pulse and a *slow* two-dimensional detector for the observation of the event (see **Figure 1**). The new concept, being developped in

collaboration between the machine division of the ESRF, CUOS in Michigan and the INRS (Institut National de Recherche Scientifique) in Montreal, will employ the standard ESRF X-ray probing pulse together with an optical laser *pumping* pulse and an ultra-fast one-dimensional detector. Such a detector is called a streak-camera.

The event itself will produce a relatively feeble photon flux to this streak camera so it needs to be repeated at an adapted frequency with the streak camera operating in a so-called accumulation mode.

The time-resolution of any time-resolving detector in accumulation mode is determined by the trigger precision, or in technical terms, the jitter. The jitter in this new concept will be made very small by triggering the streak camera using the same ultra-short laser pulse that pumps the sample, hence the name "jitter-free, accumulating streak camera".

BASIC PRINCIPLE

The principle of a streak camera is illustrated in **Figure 2**. The heart of it is the streak tube which converts the information in the time domain to a spatial domain. An X-ray impulse (duration ≈ 100 ps) will hit a photocathode which will cause the emission of photo-electrons inside the tube. This so-created electron bunch contains the same time structure as the impinging light pulse. The electrons are electrically focused and accelerated towards the other extremity of the tube where they will hit a phosphor screen. The electrons will, however, have been deflected vertically by an electric field during their transit through a pair of deflection plates. This deflection field has an ultra-fast time slope. This causes the electrons in the bunch to be deflected differently, the «first» emitted electrons will hit the phosphor screen at the bottom and the «latter» electrons higher-up. The intensity profile along the stripe-like image (a «streak») left on the phosphor screen gives the time profile of the input light impulse.

A key technique in achieving jitter-free accumulation is the triggering of the streak camera's deflection voltage ramp through a photo-conductive switch by the same laser pulse that pumps the sample, hence triggering a sub-pico second modulation on top of the X-ray pulse. This technique has been developed by the team at CUOS, University of Michigan, in Ann Arbor.

The same laboratory has built up a unique expertise in compact terawatt lasers and it is by the application of Chirped Pulse Amplification, developed at CUOS, that the necessary power levels contained in ultra-short laser pulses have become available from a device of modest dimensions.

In **Figure 3** the streak camera and its associated laser are shown in an experimental configuration. The X-ray pulses (typically 150 ps fwhm for 7-10 mA) are probing the sample at a reduced frequency from the machine orbit frequency (355 kHz). The exact value depends on the type of experiment and sample but a maximum is limited to ≈ 900 Hz by both the streak camera and the beam chopper that will be operational on ID9 beamline from spring next year.

The laser provides the optical pumping pulses at this reduced frequency with an energy of up to 25 mJ/single shot. The pulse length will be less than 200 fs. A fraction of the laser pulse energy is split off and directed to the optical switch of the streak camera deflection.

The streak camera tube being developed by the team of J-C. Kieffer at the INRS can be operated with different sweep speeds. A typical full scale time window would be 50 ps. This would be read from the phosphor screen by a CCD matrix. This device needs liquid nitrogen cooling in order to reduce its dark noise to a minimum and so permit accumulation times of the entire system of up to one hour.

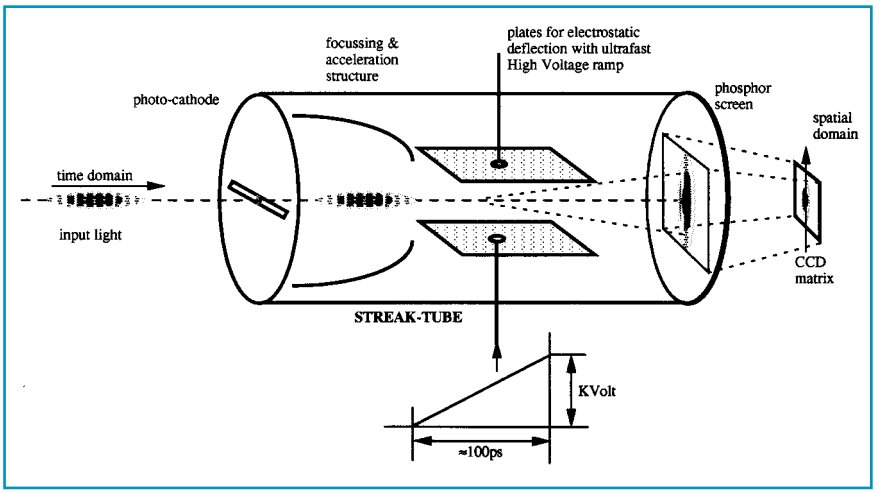

Fig. 2: Streak principle.

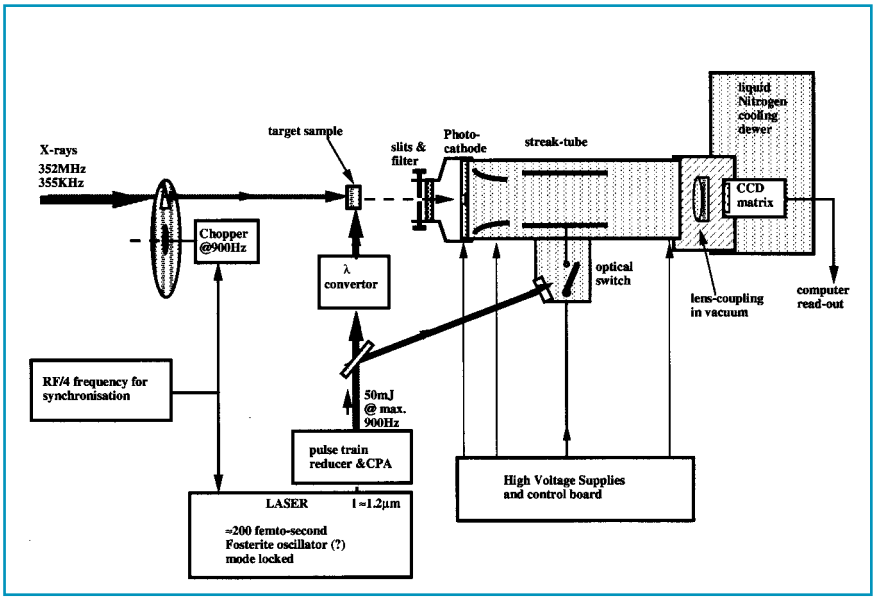

Fig. 3: Experimental configuration.

Fig. 4:
Signal read-out example.

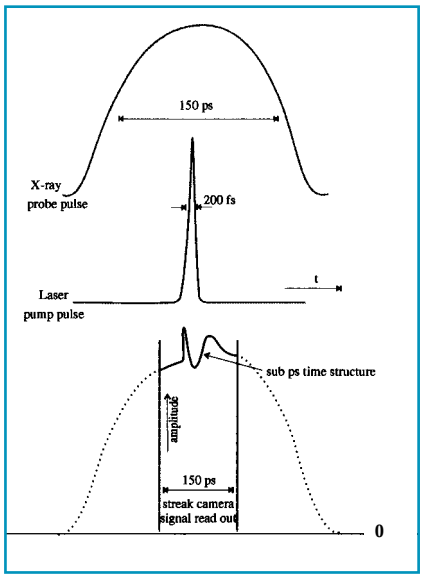

AN EXAMPLE

Three profiles in **Figure 4** present an example: the long (150 ps) X-ray probing pulse, the short (200 fs) laser pumping pulse and the signal as read by the streak camera which would show the sub-pico second time structure (triggered in the sample by the laser) as a modulation on top of the 150 ps «carrier» profile.

It can easily be shown that, in this accumulation mode, the jitter between the laser pulse and the streak deflection has to be lower than the 200 fs time-resolution which is the goal of this system. However, the jitter between the X-ray pulse and the laser pulse is less stringent and a few ps rms can be accepted. This nevertheless implies that the laser has to be mode-locked in phase with the machine light source.

At the time of writing this article the exact choice of the laser had not yet been decided. It is dependent on the wavelength requirement for the experiment as well as on energy levels and stability criteria.

COLLABORATION

The routine operation and maintenance of such a state-of-the-art laser is an important point when considering the support to be given to the future ultra-fast experiments that would become accessible with this system at the ESRF. A transfer of ultra-fast laser expertise from CUOS and the LOA (Laboratoire d'Optique Appliquée de l'ENSTA) in Paris to the ESRF is being considered.

A number of tests and milestones are defined in the collaboration contract. The first tests on a prototype are foreseen this summer at CUOS.

Tests at the ESRF throughout the three years of the project will take place on ID9 for measurements of the Detective Quantum Efficiency and time-resolution for X-ray photo-cathodes. The ID4 laboratory (UV & visible light diagnostics, Machine Division) will be permanently available for troubleshooting and verifications on linearity, jitter-free triggering, phase-locking etc. ■

References

[1] Proceedings of the 10th ICFA Beam Dynamics Panel Workshop on 4th Generation Light Sources, January 1996. Conclusions Working Group 1 - Scientific Opportunities for 4th Generation Light Sources: soft X-Rays/VUV, *Chairman I. Lindau*, **Page 23**

[2] Proceedings of the 10th ICFA Beam Dynamics Panel Workshop on 4th Generation Light Sources, January 1996. Conclusions Working Group 2 - Scientific Opportunities for 4th Generation Light Sources: hard X-Rays, *Chairman J. Als Nielsen*, **Page 33**

[3] «Ultimate brilliance of a storage ring based synchrotron radiation facility of the third generation. Potential of storage ring based third generation light source in the production of short and intense X-ray pulses (in the sub ps range)», thesis to be presented in September 1996 by C. Limborg (ESRF, Machine Division)

[4] Proceedings of the 10th ICFA Beam Dynamics Panel Workshop on 4th Generation Light Sources, January 1996. Conclusions Working Group 5 - Linac Sources, *Chairman C. Pellegrini*, **Page 57**

[5] Proceedings of the 10th ICFA Beam Dynamics Panel Workshop on 4th Generation Light Sources, January 1996. Conclusions Working Group 1 - Time-resolved Spectroscopy in the X-ray regime (ps-fs), *G. Mourou, NSF Center for Ultrafast Optical Science*, **Page WG1-25**

Events

February 1996 • Atomiades

A team of 26 ESRF members went to Radstadt (Austria) where they participated in the 6th Winteratomiade of European Research Centres. These competitions between research centres are organised every three years. These atomiades welcomed 17 research centres from 5 European countries which represented almost 400 competitors. For its first participation, many cups and medals were won by the ESRF in individual events, which meant ***the ESRF team came 3rd overall !!!***

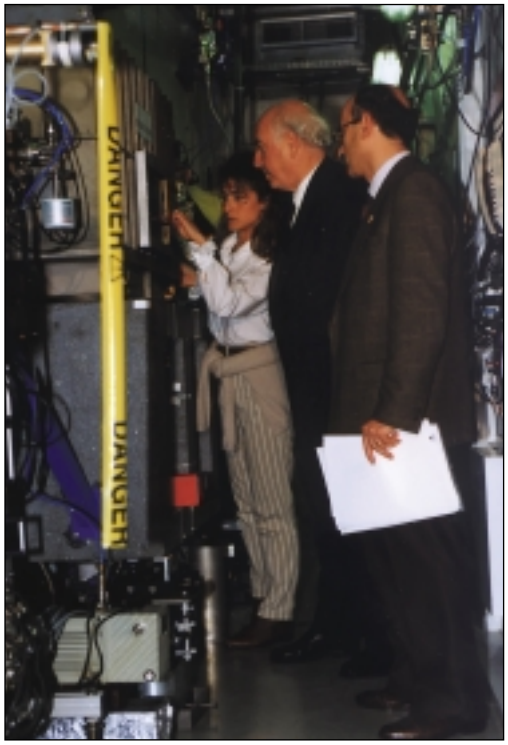

March 1996
Visit of the Italian Minister of Research

Professor Salvini (centre) listening to S. Pascarelli (left) and S. Mobilio on the Italian CRG beamline GILDA.

(See article on page 5)

18-20 November 1996
ESRF Users' Meeting: «Science at the ESRF»

(See on page 24)

The ESRF Newsletter is published by the European Synchrotron Radiation Facility
BP 220, F38043 Grenoble cedex
Editor: Dominique CORNUÉJOLS Tél (33) 76 88 20 25

Dépôt légal : 3ème trimestre 1996. Printed in France by Bastianelli. Layout by Pixel Project.